XII. Applied Mechanics

ENGINEERING MECHANICS DIVISION

A. Creep Failure of Randomly Excited Structures,

J.-N. Yang

1. Introduction

Many structures are intended to sustain, in addition to static loadings, dynamic excitations of random nature during their service life. In addition to the interior pressure, spacecraft pressure vessels are subjected to steady-state random disturbances as well as a number of severe and highly transient random excitations resulting from each flight event, such as booster engine ignition, booster engine cut-off, etc., during the mission. The investigation of creep failure under random excitations is, therefore, of practical importance as well as theoretical interest. Unfortunately, little has been done in this area, because of the lack of a unified theory to characterize the complicated phenomenon of creep rupture. Thus, in practice, in designing a spacecraft pressure vessel using the fracture mechanics approach, one takes into account the static pressure loading only, and allows for the dynamic random loadings by introducing a safety factor.

It is the purpose of this article to develop a method by which one can predict quantitatively the reliability of pressure vessels under both static loadings and random dynamic disturbances. This article establishes the relationship between the safety factor and the structural reliability, which is essential in a rational design of pressure vessels. Thus, by specifying the required level of reliability, one can determine, through this relationship, an appropriate safety factor for the design.

From the fracture mechanics viewpoint, the process of creep rupture is the slow growth of flaws in a structure, called subcritical flaw growth, until the critical fracture stress associated with the largest flaw is exceeded by the applied stress and then catastrophic failure occurs. Indeed, fracture mechanics is probably the most appropriate criterion for designing a pressure vessel (e.g., Refs. 1 and 2) and it is employed in this study. Under static sustained pressures, the characteristics of subcritical flaw growth associated with a particular material and a particular environmental condition can be obtained from the experimental results (Refs. 1 and 2). Cumulative flaw growth (or damage) hypothesis, which is analogous to the Palmgren–Miner rule, is employed to generalize the sustained flaw growth characteristics under dynamic random excitation.

The mean value and the variance of the relative flaw growth under both stationary and nonstationary random excitations are obtained where creep failure is assumed to take place when the relative flaw growth reaches unity. The probability of creep failure is then evaluated using the Janeys' principle of maximum entropy (Ref. 3).

Two numerical examples, one for stationary random excitations and another for nonstationary random excitations, are worked out to illustrate the general results. It is shown that the probability of creep failure decreases rapidly as the safety factor increases.

2. Sustained Flaw Growth Characteristics

Let A be the flaw size at some critical points of the structure. According to the well-known Griffith–Irwin equation,

$$A = Q(K_{IC}/R)^2 \tag{1}$$

$$A = Q(K_I/\underline{S})^2 \tag{2}$$

where K_{IC} is the critical stress intensity factor, R is the critical fracture stress or the resisting stress associated with the flaw size A, K_I is the stress intensity factor associated with the flaw size A and the applied stress $\underline{S}$, and Q is an appropriate state parameter (Refs. 1, 2).

Equations (1) and (2) are the basic equations relating the flaw size A to the applied stress $\underline{S}$ or the critical fracture stress R. Many structures, such as pressure vessels, fracture not only when a certain critical stress is reached but also at a relatively low stress after being subjected to a certain time of sustained loading. Such cases involve subcritical flaw growth, i.e., the slow growth of the flaw until it reaches its critical value, and then catastrophic failure occurs. The subcritical flaw growth under sustained loading can be conveniently described by curves of K_I/K_{IC} versus time to failure t_f. These curves are determined from tests on preflawed specimens by varying both the initial flaw size and the applied stress (Refs. 1, 2). Figure 1 gives typical experimental results and curves, which are available for many materials under different environmental conditions.

These experimental curves have characteristic trends indicating that, for a given material and environmental condition, practically no flaw growth occurs until a threshold value of K_I/K_{IC} is reached. In Fig. 1, this threshold value is about 0.755 for the aluminum in a nitrogen environment. It is further observed that these curves have a characteristic shape which can be approximated by

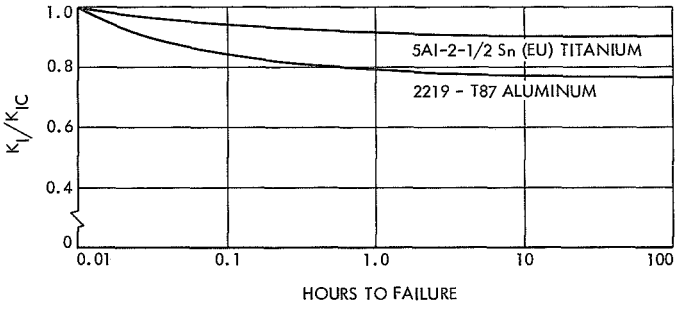

Fig. 1. Sustained load flaw growth curves for 2219-T87 aluminum and 5AI-2-½ Sn (ELI) titanium at −320°F and −423°F (Ref. 1)

an exponential decay to the threshold value (log scale in time). Thus

$$K_I/K_{IC} = b + \gamma \exp\left[-\frac{1}{\beta}\log t_f\right] = b + \gamma t_f^{-1/\alpha} \tag{3}$$

in which b is the threshold values, β is the characteristic time in logarithmic scale, $\alpha = \beta/0.43429$, $\gamma = K_I/K_{IC} - b$ for $t_f = 1$, and t_f indicates the time to fracture (failure). Note that b, γ, and α depend not only on the material properties but also on the environmental conditions, such as temperature and surrounding medium, etc.

Substitution of Eqs. (1) and (2) into Eq. (3) yields

$$\underline{S}/R = b + \gamma t_f^{-1/\alpha} \tag{4}$$

which is the relationship among the applied stress $\underline{S}$, the resisting stress of materials R (critical fracture stress), and the time to failure t_f.

3. Cumulative Flaw Growth Hypothesis

Both Eq. (4) and Fig. 1 are obtained from the experimental results under static sustained loadings. To generalize the flaw growth characteristics under dynamic or random loadings, similar assumptions as the well-known Palmgren–Miner rule are made in the following:

(1) The relative flaw growth δ_i due to a sustained stress S_i for a period of time Δt_i is given by,

$$\begin{aligned} \delta_i &= \Delta t_i/t_f(S_i), & S_i/R \geqq b \\ &= 0, & \text{otherwise} \end{aligned} \tag{5}$$

in which $t_f(S_i)$ is the time to failure under the constant sustained stress S_i (Eq. 4) and no subcritical flaw growth

is expected when K_I/K_{IC} or S_i/R is below the threshold value b.

(2) The relative flaw growth δ due to sustained stresses $S_1, S_2, \cdots, S_n$ for periods of time $\Delta t_1, \Delta t_2, \cdots, \Delta t_n$, respectively, is

$$\delta = \sum_{i=1}^{n} \delta_i = \sum_{i=1}^{n} \Delta t_i / t_f(S_i) \tag{6}$$

(3) Fracture occurs when the relative flaw growth δ reaches unity.

Let $\underline{S}(t)$ be a random stress response process with a constant mean value $\bar{S}$ and standard deviation $\sigma(t)$,

$$\underline{S}(t) = S(t) + \bar{S} \tag{7}$$

where $S(t)$ is the fluctuating part of $\underline{S}(t)$ with mean zero and standard deviation $\sigma(t)$. The mean value $\bar{S}$ represents the stress response of pressure vessels due to static pressure loadings, while $S(t)$ represents the random stress fluctuation resulting from random disturbances, such as transient excitations due to booster engine cut-off. It is further assumed that the maximum standard deviation $\sigma^*(t)$ of $S(t)$ is small compared to the mean stress response $\bar{S}$, so that the fatigue failure mode is negligible and the negative stress application of $S(t)$ can be disregarded. This assumption appears to be quite reasonable for pressure vessels.

Now define the relative flaw growth $d\delta$ due to $S(t)$ in the time interval $[t, t + dt]$ as

$$\begin{aligned} d\delta &= dt/t_f(\underline{S}(t)), && \underline{S}(t)/R \geqq b \\ &= 0, && \text{otherwise} \end{aligned} \tag{8}$$

in which no subcritical flaw growth is expected when K_I/K_{IC} or $\underline{S}(t)/R$ is below the threshold level b.

Then, the relative flaw growth $\delta(T)$ due to $\underline{S}(t)$ within the time interval $[0, T]$ follows from Eq. (8) as

$$\delta(T) = \int_0^T d\delta = \int_0^T Z(t)\, dt \tag{9}$$

where

$$\begin{aligned} Z(t) &= 1/t_f(\underline{S}(t)), && \underline{S}(t)/R \geqq b \\ &= 0, && \text{otherwise} \end{aligned} \tag{10}$$

and fracture occurs when $\delta(T)$ reaches unity.

With the aid of Eqs. (4) and (7), Eq. (10) can be written as

$$\begin{aligned} Z(t) &= C[S(t) - S_c]^\alpha, && S(t) \geqq S_c \\ &= 0, && \text{otherwise} \end{aligned} \tag{11}$$

where

$$\left.\begin{aligned} C &= (1/\gamma R)^\alpha \\ S_c &= \bar{S}(\nu - 1) \\ \nu &= bR/\bar{S} \end{aligned}\right\} \tag{12}$$

In Eq. (12), ν is the ratio of the structural resisting stress R, multiplied by the threshold level b, to the mean applied stress $\bar{S}$. In the pressure vessel design, it is called a safety factor, since for $\nu \geqq 1$, the mean applied stress $\bar{S}$, or the static pressure loading, does not produce the subcritical flaw growth and hence the creep rupture. In designing a pressure vessel, the safety factor ν is usually made greater than one, and hence $S_c \geqq 0$ to ensure that no creep failure results from the static pressure loading. Therefore, the case in which $S_c \geqq 0$ is of practical importance, and it will be assumed in the following study.

The resisting stress R, of the structure will be considered as a deterministic constant in this study. This is an approximation when the statistical dispersion of the material strength is very small. If, however, the statistical dispersion of the material strength cannot be neglected, one usually has to perform the proof load test to eliminate weak strength vessels. As a result, the proof stress is regarded as R in practice. This approximation is conservative (Refs. 4–6 and Footnote 1).

4. Mean Value and Variance of the Relative Flaw Growth

Consider the fluctuating part of the stress response $S(t)$ a gaussian process with the probability density function $f(x)$ and the joint density function $f(x, y; \rho)$,

$$f(x) = \exp(-x^2/2\sigma_1^2)/\sqrt{2\pi}\,\sigma_1 \tag{13}$$

$$f(x, y; \rho) = \frac{1}{2\pi\sigma_1\sigma_2(1-\rho^2)^{1/2}} \exp\left\{-\frac{x^2 - 2\rho xy + y^2}{2\sigma_1\sigma_2(1-\rho^2)}\right\} \tag{14}$$

[1]Heer, E., and Yang, J.-N., "Structural Optimization Based on Fracture Mechanics and Reliability Criteria," to appear in *AIAA Journal*.

where

$$\sigma_1^2 = \sigma_1^2(t_1) = E[S^2(t_1)]$$
$$\sigma_2^2 = \sigma_2^2(t_2) = E[S^2(t_2)]$$
$$\rho\sigma_1\sigma_2 = \rho(t_1, t_2)\,\sigma_1(t_1)\,\sigma_2(t_2) = E[S(t_1)\,S(t_2)]$$

If $S(t)$ is stationary, $\sigma_1 = \sigma_2 = \sigma_s$ = constant and $\rho(t_1, t_2) = \rho(t_1 - t_2) = \rho(\tau)$.

Following Cramer (Ref. 7), $f(x, y; \rho)$ can be expanded into a series,

$$f(x, y; \rho) = \frac{1}{\sigma_1\sigma_2}\sum_{n=0}^{\infty}\frac{\rho^n}{n!}\Phi^{(n+1)}\left(\frac{x}{\sigma_1}\right)\Phi^{(n+1)}\left(\frac{y}{\sigma_2}\right) \tag{15}$$

in which $\Phi(x)$ is the standardized gaussian distribution function and $\Phi^{(n)}(x)$ is the nth derivative of $\Phi(x)$ with respect to x.

a. Stationary random excitation. When $S(t)$ is stationary with standard deviation σ_s, the mean value, $\bar{\delta}(T)$, of the relative flaw growth, $\delta(T)$, within the time interval $[0, T]$, follows from Eqs. (9), (11), and (13) as

$$\bar{\delta}(T) = E[\delta(T)] = \int_0^T E[Z(t)]\,dt$$
$$= TC\int_{S_c}^{\infty}(x - S_c)^{\alpha} f(x)\,dx \tag{16}$$

With the aid of Eq. (12), one obtains

$$\bar{\delta}(T) = T(C\sigma_s^{\alpha})\frac{1}{\sqrt{2\pi}}\exp(-\lambda^2/4)\,\Gamma(\alpha + 1)\,D_{-(\alpha'+1)}(\lambda) \tag{17}$$

in which $\Gamma(\cdot)$ and $D(\cdot)$ are, respectively, the gamma function and the parabolic cylinder function, and

$$\lambda = S_c/\sigma_s = \bar{S}(v - 1)/\sigma_s = (v - 1)/V$$
$$C\sigma_s^{\alpha} = (\sigma_s/\gamma R)^{\alpha} = (Vb/\gamma v)^{\alpha} \tag{18}$$

where

$$V = \sigma_s/\bar{S} \tag{19}$$

is the coefficient of variation of $\underline{S}(t)$.

For the special case in which $v = 1.0$ and hence $S_c = 0$, one can show that

$$\bar{\delta}(T) = T(C\sigma_s^{\alpha})(2)^{\alpha/2}\,\Gamma\frac{1}{2\sqrt{\pi}}T(C\sigma_s^{\alpha})(2)^{\alpha/2}\cdot\Gamma\left(\frac{\alpha}{2} + \frac{1}{2}\right) \tag{20}$$

Therefore, the average time to fracture (creep failure) T^* follows from Eq. (17) as

$$T^* = \sqrt{2\pi}/(C\sigma_s^{\alpha})\exp(-\lambda^2/4)\,\Gamma(\alpha + 1)\,D_{-(\alpha+1)}(\lambda) \tag{21}$$

The variance, $\sigma^2_{\delta(T)}$, of $\delta(T)$ can be obtained from Eqs. (9), (11), (14) and (17) as

$$\sigma^2_{\delta(T)} = C^2\int_0^T\int_0^T\int_{S_c}^{\infty}\int_{S_c}^{\infty}(x - S_c)^{\alpha}(y - S_c)^{\alpha} f(x, y; \rho)\,dx\,dy\,dt_1\,dt_2 - \bar{\delta}^2(T) \tag{22}$$

Substituting Eqs. (15) and (17) into Eq. (22) and inverting the order of integration and summation, one can show that the first term associated with $n = 0$ is cancelled by the term $\bar{\delta}^2(T)$. For α = integer, using the stationary condition and repeating the integration by parts with respect to each term of the series, one can show that

$$\sigma^2_{\delta(T)} = 2T(C\sigma_s^{\alpha})^2(\alpha!)^2\left\{\sum_{j=1}^{\alpha}\frac{G(j; T)\,F^2(j, \lambda)}{j!\,[(\alpha - j)!]^2} + \sum_{j=1}^{\infty}\frac{G(j + \alpha; T)\,H^2_{j-1}(\lambda)\,\phi^2(\lambda)}{(\alpha + j)!}\right\} \tag{23}$$

in which

$$F(j,\lambda)=\frac{1}{\sqrt{2\pi}}\exp\left(\frac{-\lambda^2}{4}\right)\Gamma(\alpha-j+1)\,D_{-(\alpha-j+1)}(\lambda) \tag{24}$$

$$G(j;T)=\int_0^T\left(1-\frac{\tau}{T}\right)\rho^j(\tau)\,d\tau \tag{25}$$

where H and ϕ are, respectively, the Hermit polynomial and the standardized gaussian density function. The relationship

$$\Phi^{(j+1)}(x)=(-1)^j H_j(x)\,\phi(x) \tag{26}$$

has been employed in deriving Eq. (23).

In statistical terminology, the random variable of the relative flaw growth $\delta(T)/C$ is called "exceedance measure" (Ref. 7). It can be observed from Eqs. (9) and (11) that, for $\alpha=0$, $\delta(T)/C$ is the proportion of time in $[0,T]$ that the fluctuating process $S(t)$ spends above the level S_c. For $\alpha=1$, $\delta(T)/C$ is just the area cut off by the process $S(t)$ above the level S_c in $[0,T]$ as shown in Fig. 2.

The correlation coefficient $\rho(\tau)$ usually dies down to zero as τ becomes large, so that $\rho(\tau)\approx 0$ for $\tau\geqq t^*$, say, e.g., $t^*=10$ min. In practice, one is usually interested in the creep failure for $T>>t^*$, say, e.g., $T>1$ h. Hence, $G(j;T)$ in Eq. (25) can be approximated by

$$G(j;T)\approx G(j)=\int_0^{t^*}\rho^j(\tau)\,d\tau=\int_0^{\infty}\rho^j(\tau)\,d\tau \tag{27}$$

which is not a function of T.

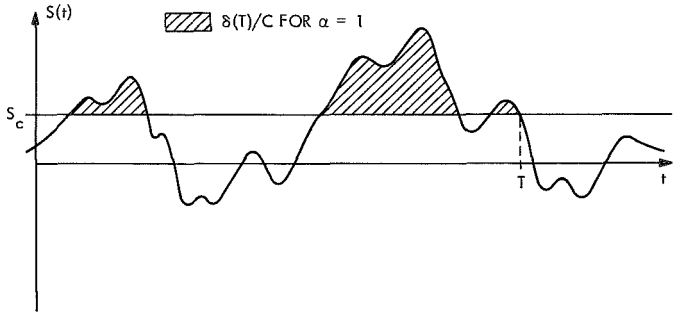

Fig. 2. Measure of relative flaw growth $\delta(T)/C$ for $\alpha=1$

Therefore, for large T, the standard deviation, $\sigma_{\delta(T)}$, increases in proportion to the square root of T. It follows from Eqs. (17), (23) and (27) that the coefficient of variation (dispersion), $V_{\delta(T)}$, of the relative flaw growth $\delta(T)$ can be expressed as

$$V_{\delta(T)}\sim\frac{W}{\sqrt{T}}\qquad \text{as } T\to\text{large} \tag{28}$$

where

$$W=\frac{2\sqrt{\pi}\,(\alpha!)}{\exp\left(-\frac{\lambda^2}{4}\right)\Gamma(\alpha+1)\,D_{-(\alpha+1)}(\lambda)}\times\left\{\sum_{j=1}^{\alpha}\frac{G(j)\,F^2(j,\lambda)}{j!\,[(\alpha-j)!]^2}+\sum_{j=1}^{\alpha}\frac{G(j+\alpha)\,H_{j-1}^2(\lambda)\,\phi^2(\lambda)}{(\alpha+j)!}\right\}^{1/2} \tag{29}$$

Equation (28) states that the dispersion of $\delta(T)$ decreases in inversed proportion to the square root of T.

b. Nonstationary random excitations. When $S(t)$ is a nonstationary gaussian process, the standard deviation $\sigma(t)$, is a function of time and the correlation coefficient $\rho(t_1,t_2)$ depends on t_1 and t_2. In a similar fashion as for the stationary process, one can show that the mean value of $\delta(T)$ is

$$\bar{\delta}(T)=C\int_0^T\int_{S_c}^{\infty}(x-S_c)^{\alpha}f(x)\,dx$$

$$=(CS_c)^{\alpha}\frac{\Gamma(\alpha+1)}{\sqrt{2\pi}}\int_0^T\left(\frac{\sigma(t)}{S_c}\right)^{\alpha}\exp\left\{-\left(\frac{S_c}{2\sigma(t)}\right)^2\right\}\times D_{-(\alpha+1)}\left(\frac{S_c}{\sigma(t)}\right)dt \tag{30}$$

in which

$$(CS_c)^{\alpha}=[b(\nu-1)/\gamma\nu]^{\alpha} \tag{31}$$

The variance $\sigma^2_{\delta(T)}$ can be obtained from Eq. (22) as follows: after substituting Eqs. (15) and (30) into Eq. (22) and inverting the order of integration and summation,

one repeats the integration by parts for each term of the series to yield, for α = integer,

$$\sigma^2_{\delta(T)} = (CS_c)^{2\alpha}(\alpha!)^2 \int_0^T \int_0^T \left(\frac{\sigma_1}{S_c}\right)^\alpha \left(\frac{\sigma_2}{S_c}\right)^\alpha \times \left\{ \sum_{j=1}^{\alpha} \frac{\bar{F}(j; t_1)\,\bar{F}(j; t_2)}{j!\,[(\alpha - j)!]^2} \rho^j(t_1, t_2) + \sum_{j=1}^{\infty} \frac{\rho^{j+\alpha}(t_1, t_2)}{(\alpha + j)!} H_{j-1} \times \left(\frac{S_c}{\sigma_1}\right) H_{j-1}\left(\frac{S_c}{\sigma_2}\right) \phi\left(\frac{S_c}{\sigma_1}\right) \phi\left(\frac{S_c}{\sigma_2}\right) \right\} dt_1\, dt_2 \tag{32}$$

where

$$\bar{F}(j; t_1) = \exp\left\{-\left(\frac{S_c}{2\sigma_1}\right)^2\right\} \Gamma(\alpha - j + 1)\, D_{-(\alpha - j + 1)} \times \left(\frac{S_c}{\sigma_1}\right) \Big/ \sqrt{2\pi} \tag{33}$$

5. Probability of Failure

With the mean value $\bar{\delta}(T)$ and the variance $\sigma^2_{\delta(T)}$ computed in the previous section, the probability of creep failure can be estimated using the Janeys' principle of maximum entropy (Ref. 3). Since creep failure occurs when $\delta(T)$ reaches unity, the probability of creep failure $P_f(T)$ within the time interval $[0, T]$ can be shown (Ref. 3) as

$$P_f(T) = \exp\left(-1/\bar{\delta}(T)\right) \tag{34}$$

when only the information of $\bar{\delta}(T)$ is available. If both $\delta(T)$ and $\sigma^2_{\delta(T)}$ are given, $P_f(T)$ can be shown as

$$P_f(T) = \frac{2}{\sqrt{\pi}} \int_1^\infty \exp\left(-a_0 - a_1 x - a_2 x^2\right) dx = \frac{1}{\sqrt{a_2}} \exp\left\{-a_0 + \frac{a_1^2}{4a_2}\right\} \operatorname{erfc}\left(\sqrt{a_2} + \frac{a_1}{2\sqrt{a_2}}\right) \tag{35}$$

with

$$\left.\begin{aligned} a_1 &= (Z - 2X^2)/\bar{\delta}(T) \\ a_2 &= a_1^2/4X^2 \\ a_0 &= (a_1^2/4a_2) - \frac{1}{2}\ln a_2 + \ln\left[\operatorname{erfc}\left(\frac{a_1}{2\sqrt{a_2}}\right)\right] \end{aligned}\right\} \tag{36}$$

where X and Z appearing in above equations can be obtained graphically from the following equations

$$Z = 2X \exp(-x^2)/\sqrt{\pi}\operatorname{erfc}(X)$$
$$\sigma^2_{\delta(T)}/\bar{\delta}^2(T) = (2X^2 + 2X^2Z - Z^2)/(4X^4 - 4X^2Z + Z^2) \tag{37}$$

In Eqs. (35) and (37), erfc $(\cdot)$ represents the complimentary error function.

6. Numerical Examples

Consider the displacement response $Y(t)$, of a structure which is related to the excitation $g(t)$, as follows:

$$\ddot{Y}(t) + 2\zeta\omega_0\dot{Y}(t) + \omega_0^2 Y(t) = g(t) \tag{38}$$

where ζ and ω_0 are, respectively, the damping coefficient and the natural frequency of the structure. The stress response process $S(t)$ is linearly related to the displacement response $Y(t)$ as

$$S(t) = KY(t) \tag{39}$$

where K is a suitable constant. In addition to the excitation $g(t)$, the structure is also subjected to a deterministic static loading which produces a static stress $\bar{S}$ in the structure.

The subcritical flaw growth characteristics of Fig. 1 for 2219-T87 aluminum is employed in this example. This curve can be fitted accurately by the following set of parameter values appearing in Eq. (3); $b = 0.755$, $\gamma = 0.038$, $\alpha = 2.5$.

Example 1: Let $g(t)$ be a stationary white noise $n(t)$ with a mean square spectral density S_0. Then the standard deviation, σ_s, of the stress response $S(t)$ is

$$\sigma_s = K(\pi S_0/2\zeta\omega_0^3)^{1/2} \tag{40}$$

and the correlation coefficient $\rho(\tau)$ is

$$\rho(\tau) = \exp(-\zeta\omega_0\tau)\left[\cos\omega\tau + \frac{\zeta}{\sqrt{1-\zeta^2}}\sin\omega\tau\right] \qquad (41)$$

where

$$\omega = \sqrt{1-\zeta^2}\,\omega_0$$

It is assumed that $\omega_0 = 2$ rad/s, $\zeta = 0.02$ and the coefficient of variation $V = \sigma_s/\bar{S} = 0.05$. It can be observed that $\rho(\tau)$ becomes negligible for $\tau > 10$ min and hence $G(j)$ appearing in Eq. (27) can be used in approximation for $T > 1$ h.

It is now possible to find the mean value $\bar{\delta}(T)$ (Eq. 17) and the standard deviation $\sigma_{\delta(T)}$ (Eq. 23) of the relative flaw growth as functions of safety factor ν and time T. The average flaw growth per hour, $\bar{\delta}(T)/T$, and the measure of the coefficient of variation, $W = V_{\delta(T)}\sqrt{T}$ (Eq. 28), with $G(j)$ given in Eq. (27), are plotted against ν in Fig. 3 as the solid and dashed curves, respectively. From Fig. 3, $\bar{\delta}(T)$ and $\bar{\delta}(T) \pm 3\sigma_{\delta(T)}$ can be plotted against time T for different values of ν and is shown in Fig. 4, in which T^* represents the average time to failure. It can be observed that T^* increases rapidly with respect to the increase of the safety factor. The criterion for failure is $\delta(T) = 1$. Fig. 4 indicates that, given a specific time instant T, there is a distribution of $\delta(T)$ across the ensemble of sample histories. The probability of failure can, therefore, be computed using the principle of maximum entropy (Eq. 35) and is plotted in Fig. 4 (dotted curves).

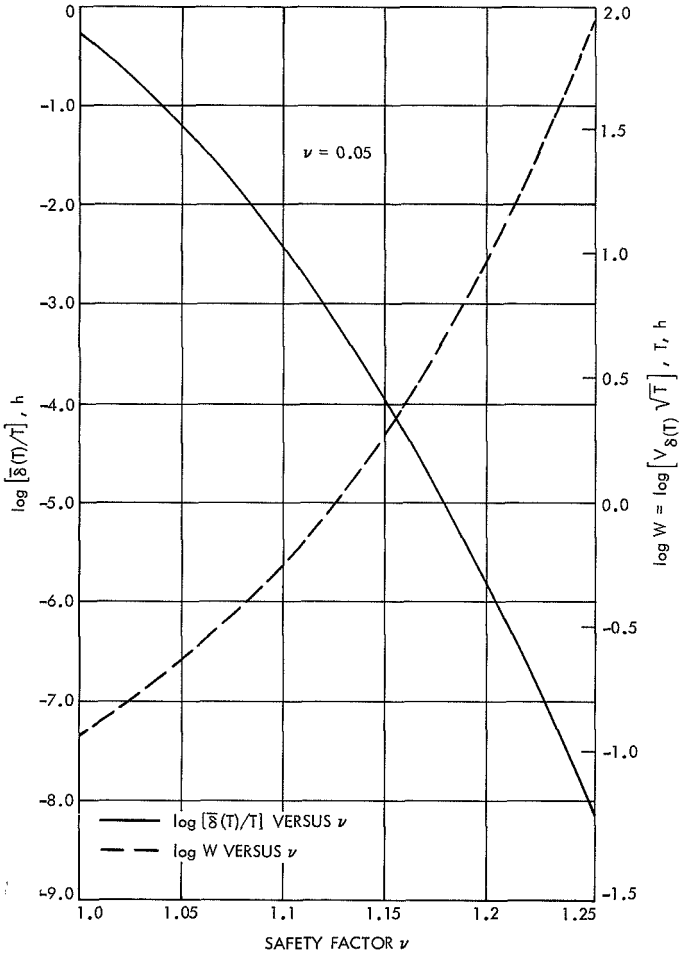

Fig. 3. Expected relative flaw growth per hour, $\bar{\delta}(T)/T$ and measure of dispersion $V_{\delta(T)}\sqrt{T}$ as function of safety factor ν

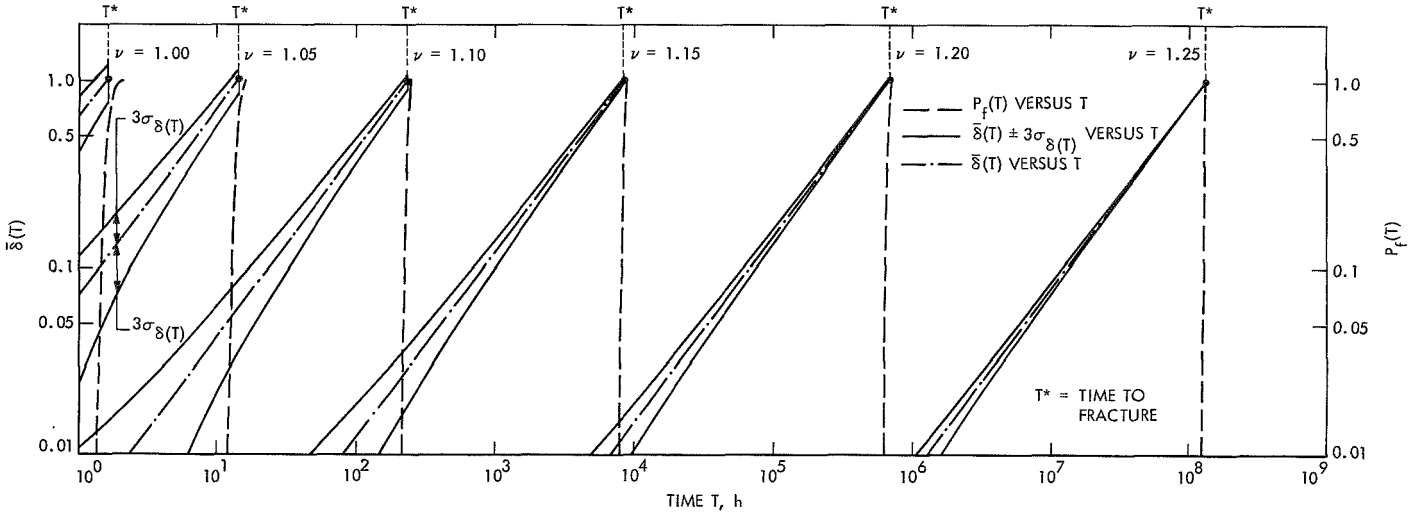

Fig. 4. Expected relative flaw growth $\bar{\delta}(T)$, $\bar{\delta}(T) \pm 3\sigma_{\delta(T)}$, and probability of failure $P_f(T)$ as function of time T

Example 2: Nonstationary Random Excitation

Consider the same structure (Eq. 38) where, however, $\omega_0 = 31.4$ rad/sec $\zeta = 0.05$, and the excitation $g(t)$ is a nonstationary random process obtained as an output of a filter due to a nonstationary shot noise $\psi(t)\, n(t)$ with $\psi(t)$ being a deterministic function of time,

$$g(t) = \int_{-\infty}^{\infty} h_0(t-\tau)\,\psi(\tau)\,n(\tau)\,d\tau \tag{42}$$

$$\psi(t) = H(t)\,[e^{-\beta_1 t} - e^{-\beta_2 t}] \qquad (\beta_2 > \beta_1 > 0) \tag{43}$$

$$h_0(t) = H(t)\,[e^{-\mu_b t}\sin\omega_b t]/\omega_b \tag{44}$$

in which $h_0(t)$ is the impulse response function of the filter, $H(t)$ is a unit step function, and $n(t)$ is a white noise with a mean square spectral density S_0. The significance and the application of the input $g(t)$ given in Eq. (42) was discussed in detail in Ref. 8. It is pointed out here that by a proper choice of parameter values involved, $g(t)$ can represent a strong earthquake acceleration or a severe transient gust loading.

Using Eqs. (38) and (42) to (44), the variance $\sigma^2(t)$ and the correlation coefficient $\rho(t_1, t_2)$, of the stress response process $S(t)$ can be obtained (Ref. 9). In the present example, a choice of parameter values, which has been employed to investigate the first-excursion probability (Ref. 8) and the cumulative fatigue damage (Ref. 10), is used as follows: $\beta_1 = 0.25$/sec, $\beta_2 = 0.5$/sec, $\omega_b = 12.3$ rad/sec, $\mu_b = 3.86$/sec, and $S_0 = 7.19 \times 10^4$ in./sec. It is further assumed that $K/R = 3.0$ per inch. With this set of parameter values, $g(t)$ represents a transient excitation which dies down to zero after $t \geqq 15$ sec (Refs. 8, 9, Footnote 2). The mean value of the relative flaw growth (Eq. 30), denoted by $\bar{\delta}$ for $T \geqq 15$ sec, is computed for different value of safety factor ν and plotted in Fig. 5 as the solid curve. The probability of creep failure is then computed using Eq. (34) and plotted in Fig. 5 as the dashed curve. The results of Fig. 5 indicate that the probability of creep failure decreases rapidly as the safety factor increases. It is worthwhile to note that, in practice, a safety factor $\nu = 1.25$ is used in designing spacecraft pressure vessels indicating a high level of reliability.

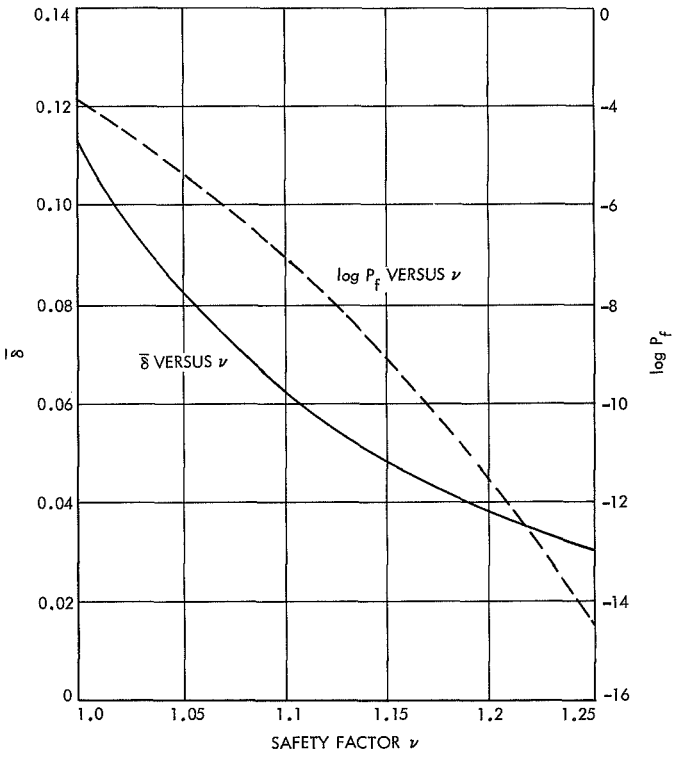

Fig. 5. Expected relative flaw growth $\bar{\delta}$ and probability of failure P_f as function of safety factor ν (nonstationary random excitation)

References

1. Tiffany, C. F., Masters, J. N., and Pall, F. A., *Some Fracture Considerations in Design and Analysis of Spacecraft Pressure Vessels*, ASM Technical Report C6-2.3, 1966.

2. Masters, J. N., "Cyclic and Sustained Flaw Growth Characteristics of 6Al-4V Titanium," NASA CR-92231, July, 1968.

3. Tribus, M., "The Use of Maximum Entropy Estimate in the Estimation of Reliability," in *Recent Developmcnt in Information and Decision Processes*, pp. 102–140. Edited by R. E. Machol and P. Gray, Macmillan Co., New York, 1962.

4. Shinozuka, M., and Yang, J.-N., "Optimum Structural Design Based on Reliability and Proof Load Test," *Annals of Assurance Science*, Vol. 8, pp. 375–391, 1969.

5. Shinozuka, M., Yang, J.-N., and Heer, E., "Optimum Structural Design Based on Reliability Analysis," *Proceedings of the Eighth International Symposium on Space Technology and Sciences*, pp. 245–258, Tokyo, Japan, Aug. 1969.

[2]Shinozuka, M., and Yang, J.-N., "Peak Structural Response to Nonstationary Random Excitations," accepted to appear in *Journal of Sound and Vibration*.

6. Heer, E., and Yang, J.-N., "Optimum Pressure Vessel Design Based on Fracture Mechanics and Reliability Criteria," *Proceedings of the ASCE-EMD Specialty Conference on Probabilistic Concepts and Methods in Engineering*, pp. 102–106, Purdue University, Nov. 1969.
7. Cramer, H., and Leadbetter, M. R., *Stationary and Related Stochastic Process*, John Wiley and Sons, Inc., New York, 1967.
8. Shinozuka, M., and Yang, J.-N., "On the Bound of First-Excursion Probability," *J. EMD, Proc. ASCE*, Vol. 95, pp. 363–377, 1969.
9. Shinozuka, M., and Yang, J.-N., "Random Vibration of Linear Structures," *Int. J. Solids and Structures*, Vol. 5, pp. 1005–1036, Oct. 1969.

B. Reliability of Randomly Excited Structures,

J.-N. Yang and E. Heer

1. Introduction

Structural reliability under random excitations is a well-recognized problem in aerospace engineering. In-flight measurements taken during the launch and exit phase of recent space flights (Ref. 1) show that spacecraft excitations and responses contain to a large degree steady-state random components in addition to certain deterministic phenomena. Aircraft structural loads and excitations as a result of engine noise and boundary layer turbulence are usually also classified as stationary random. The requirement of studying structural reliability and failure under stationary random excitations is therefore apparent.

Because of mathematical expediency, three essential modes of structural failure are usually investigated separately: catastrophic, fatigue, and creep.

a. Catastrophic failure. This type occurs instantaneously due to some response measures, such as displacements or stresses, that exceed their limiting values. This type of failure is also referred to as the first passage failure, and the associated probability of catastrophic failure is called the first passage or the first excursion probability. Although, the exact solution for a simple structural system excited by white noise has not been obtained (Ref. 2) many approximate solutions have been proposed (Refs. 3–4, Footnote 1).

b. Fatigue failure. This type occurs due to the successive incremental reduction of the limiting response measures as a result of flaw extension with each load repetition. Fatigue failure estimations are usually made using the well-known Palmgren–Miner rule, e.g., Refs. 5, 6, or using the fracture mechanics approach, e.g., Ref. 7.

c. Creep failure. This type occurs due to the continuous time-dependent reduction of the limiting response measures as a result of viscous flow phenomena in each sustained loading time interval. Very little information is available for the estimation of creep failures under random excitation.

Thus far, in random vibration, the material properties of structures have not been considered as random variables, and the relevancy of structural reliability to optimum structural design has not been investigated thoroughly. On the other hand, structural reliability under static or quasistatic random loadings, taking into account statistical variations of material properties, has been investigated quite extensively. The relevancy of structural reliability, coupled with proof testing and structural strength deterioration (fatigue and creep), to optimum structural design has been investigated, e.g., in Refs. 8–10 and Footnote 2.

In this article, the concepts of fracture mechanics and the point processes associated with stationary narrow-band random processes (Footnote 1) are employed to estimate the reliability of structures under stationary random excitations. Two failure modes are allowed for, i.e., catastrophic and fatigue failures, and the statistical variations of the material properties are taken into account. A quantitative investigation is conducted to determine the interaction of the failure modes and the relevancy to structural reliability estimates. The premises of this study are as follows: (1) catastrophic failure occurs as soon as the stress response process exceeds the critical

[1]Yang, J.-N., and Shinozuka, M., "On the First Excursion Probability in Stationary Narrow-Band Random Vibration," to appear in the *Journal of Applied Mechanics*.

[2]Heer, E., and Yang, J.-N., "Structural Optimization Based on Fracture Mechanics and Reliability Criteria," to appear in the *AIAA Journal*.

fracture stress (threshold level) of the structure, and (2) successive incremental reduction of the critical fracture stress (threshold level), as a result of stress repetition, increases the catastrophic failure rate in time. Therefore, the problem treated here is a first passage problem with a monotonically decreasing probabilistic barrier level that depends not only on the dispersion of the material properties but also on the history of the random response process.

2. Strength Deterioration of Structures

One way of explaining structural failure mechanisms and processes, such as fatigue failures is by the use of the concepts of fracture mechanics. The mechanisms of fatigue failure can then be summarized as follows: (1) flaw initiation, (2) flaw propagation, and (3) catastrophic failure. The last two mechanisms of the fatigue process are of primary concern in structural analysis and design. The flaw initiation stage is the one about which little is known at present. It can usually be assumed, however, that the material already has flaws that propagate under repetitive stress applications with sufficiently high amplitude. The fatigue failure process is thus described by the growth of flaws in a structure until the applied stress at any flawed point exceeds the critical fracture stress associated with the flaw at that critical point, and catastrophic failure occurs.

Let A represent the flaw size at the critical point of the structure. According to the well-known Griffith–Irwin equation

$$A = Q\left(\frac{K_{IC}}{R}\right)^2 \tag{1}$$

$$A = Q\left(\frac{K_I}{S}\right)^2 \tag{2}$$

where K_{IC} is the critical stress intensity factor, R is the critical fracture stress or the resisting stress associated with the flaw size A, K_I is the stress intensity factor associated with the flaw size A and the applied stress S, and Q is an appropriate state parameter.

The flaw propagation law takes the form (Refs. 7, 11–12)

$$\frac{dA}{dn} = C K_I^b \tag{3}$$

stating that the rate of flaw extension with respect to the number of stress cycles n is proportional to the bth power of the stress intensity factor K_I, where C is a suitable constant. By theoretical analyses as well as direct measurements of flaw propagations (Refs. 7, 11, 12) it has been shown that b ranges from 2 to 4, depending on the material used and environmental conditions such as temperature, corrosion, etc.

Substituting Eq. (2) into Eq. (3), one obtains

$$\frac{dA}{dn} = K S^b A^{b/2} \tag{4}$$

where $K = C/Q^{b/2}$ is a constant.

In the following approach, it is assumed, for convenience and without essential loss of generality, that $b = 2$; it will be shown later that this applies also to the cases $b = 3$ or 4. Note that b is held arbitrary for S, which is a parameter in Eq. (4).

Integrating Eq. (4) successively with respect to each cycle and summing, one obtains

$$\ln A_n - \ln A_0 = K \sum_{j=1}^{n} S_j^b \tag{5}$$

where S_j is the jth peak of the stress response $S(t)$. The initial flaw size, A_0, and the flaw size after n stress cycles, A_n, are respectively related to the initial resisting stress, R_0, and the resisting stress after n stress cycles, R_n, through Eq. (1). Hence, substituting Eq. (1) into Eq. (5) yields

$$R_n = R_0 \exp(-Z) \tag{6}$$

$$Z = \frac{1}{2} K \sum_{j=1}^{n} S_j^b \tag{7}$$

It is clear from Eqs. (6) and (7) that the structural resisting stress after n stress cycles, R_n, decreases monotonically with respect to the number of stress cycles n.

3. Extreme Point Processes

Consider $S(t)$ a stationary narrow-band gaussian stress response process with mean zero and a mean square spectral density $\phi(\omega)$. If S_m denotes the mth local maximum (peak) of $S(t)$, then the local maxima form a stationary point process called the maximum point process, $\{S_n\}$ (Footnote 1).

The distribution function $F_{S_n}(x)$ of the maximum point process $\{S_n\}$ is the Rayleigh distribution

$$F_{S_n}(x) = 1 - \exp\left\{\frac{-x^2}{2\sigma_S^2}\right\} \tag{8}$$

in which σ_S is the standard deviation of $S(t)$.

Because of the narrow-band characteristics of $S(t)$, the joint density function

$$f_{S_j S_{j+m}}(x, y)$$

of S_j and S_{j+m} spaced at a distance of m cycles can be approximated by the joint density function $f_S(x, y; \tau)$ of the envelope function of $S(t)$ spaced at a distance $\tau = mT_0$, where T_0 is the central period of $S(t)$.

$$f_{S_j S_{j+m}}(x, y) = f_S(x, y; mT_0) \tag{9}$$

It has been shown in Ref. 13 that

$$f_S(x, y; \tau) = \frac{xy}{\sigma_S^4[1 - k_0^2(\tau)]} \times I_0\left[\frac{xy\,k_0(\tau)}{\sigma_S^2[1 - k_0^2(\tau)]}\right] \exp\left\{\frac{-(x^2 + y^2)}{2\sigma_S^2[1 - k_0^2(\tau)]}\right\} \tag{10}$$

in which $I_0[\cdot]$ is the zero-order modified Bessel function of the first kind, and $k_0(\tau)$ is a function of $\phi(\omega)$ and its central frequency ω_0 (Footnote 1).

4. Failure Rate and Reliability

The probability that a structure, having survived n stress cycles, will fail in the $(n + 1)$th stress cycle is denoted by $h(n)$ and is called failure rate, risk function, or hazard function, i.e.,

$$h(n) = P\left[R_n \leqq S_{n+1} \,\middle|\, \bigcap_{j=1}^{n} (R_{j-1} > S_j)\right]; \qquad n = 1, 2, \cdots \tag{11}$$

$$h(0) = P[R_0 \leqq S_1]$$

where R_n is given by Eq. (6).

The probability that the structure will survive N stress cycles, denoted by $L(N)$, is called reliability. Successive application of Eq. (11) yields

$$L(N) = \prod_{n=0}^{N-1} [1 - h(n)] \tag{12}$$

and for $h(n) << 1$, a conservative good approximation can be obtained as

$$L(N) \simeq \exp\left\{-\sum_{n=0}^{N-1} h(n)\right\} \tag{13}$$

a. Poisson approximation: If the point process $\{S_n\}$ is assumed to be of Poisson type (Footnote 1), i.e., S_{n+1} is independent of $S_j; j=i, 2, \cdots, n$ and the event $\{R_n \leqq S_{n+1}\}$ is independent of the past event

$$\left\{\bigcap_{j=1}^{n} (R_{j-1} > S_j)\right\}$$

then the Poisson failure rate $h_p(n)$ follows from Eq. (11) as

$$h_p(n) = P[R_n \leqq S_{n+1}] = \int_0^\infty [1 - F_{S_{n+1}}(x)]\, f_{R_n}(x)\, dx \tag{14}$$

in which $f_{R_n}(x)$ and $F_{S_{n+1}}(x)$ are, respectively, the probability density function of R_n and the distribution function of S_{n+1} given in Eq. (8).

Eq. (6) can be written as follows:

$$\ln R_n = \ln R_0 - Z \tag{15}$$

The statistical distribution of the initial resisting stress R_0 is determined by material specimen tests, the form of which is a material characteristics and reflects environmental conditions. Experience shows that the normal, log normal, gamma or Weibull distribution can be applied in most cases. Using the log-normal distribution for R_0 because of simplicity and because it is quite reasonable for many engineering materials, the term $\ln R_0$ in Eq. (15) is normally distributed.

It is observed from Eq. (7) that Z is the sum of dependent random variables $S_j^b; j = 1, 2, \cdots, n$. As will be

shown later, the distribution of Z is asymptotically normal. Therefore, for large n, the distribution of Z can reasonably be approximated by the normal distribution. Furthermore, we shall restrict ourselves to the case of high-cycle fatigue where the average number of cycles to failure is large. Hence, the effect of Z (fatigue failure mode) on the failure rate $h_p(n)$, see Eqs. (14), (6), and (7), is negligible for small values of n. Therefore, the distribution of Z for small n is irrelevant to the reliability estimate. As a result, the distribution of Z is approximated by the normal distribution. It therefore follows from Eq. (15) that $\ln R_n$ is also normally distributed with the mean value μ_n and the variance σ_n^2 given by:

$$\mu_n = \mu_0 - \mu_z$$
$$\sigma_n^2 = \sigma_0^2 + \sigma_z^2 \tag{16}$$

where μ_0 and σ_0^2 are the mean value and the variance, respectively, of the normal random variable $\ln R_0$. The mean value μ_z and the variance σ_z^2 of Z can be computed using Eqs. (7), (8) and (10). The results are as follows:

$$\mu_z = \frac{n}{2} K(\sqrt{2}\sigma_S)^b \Gamma\left(1 + \frac{b}{2}\right) \tag{17}$$

$$\sigma_z^2 = \frac{n}{4} K^2 (\sqrt{2}\sigma_S)^{2b}\left[\Gamma(1+b) - \Gamma^2\left(1+\frac{b}{2}\right)\right] + \frac{1}{4} K^2 (\sqrt{2}\sigma_S)^{2b} \tag{18}$$

$$\Gamma^2\left(1+\frac{b}{2}\right)\left\{\sum_{m=1}^{n-1}(n-m)\left[{}_2F_1\left(-\frac{b}{2}, -\frac{b}{2}; 1, k_0^2(mT_0)\right) - 1\right]\right\}$$

$$E[S_j^b S_{j+m}^b] = (\sqrt{2}\sigma_S)^{2b}\Gamma^2\left(1+\frac{b}{2}\right) {}_2F_1\left(-\frac{b}{2}, -\frac{b}{2}; 1, k_0^2(mT_0)\right) \tag{19}$$

where $\Gamma[\cdot]$ and ${}_2F_1(\cdot)$ are, respectively, the gamma function and the hypergeometric function, and $E[\cdot]$ denotes the expectation. Further evaluation of σ_z^2 requires a specific choice for the mean square spectral density of the response process $S(t)$ in order to specify the parameter $k_0^2(mT_0)$ and hence the hypergeometric function.

For a single-degree-of-freedom oscillator under white noise excitation, Crandall et al., (Ref. 5) obtained the following simplified expressions for σ_z^2 when the damping coefficient ζ is small and when b is odd:

$$\sigma_z^2 = \frac{n}{4\zeta} K^2(\sqrt{2}\sigma_S)^{2b}\Gamma^2\left(1+\frac{b}{2}\right) f_1(b) \tag{20}$$

$$V_z = \left[\frac{f_1(b)}{n\zeta}\right]^{1/2} \tag{21}$$

where V_z is the coefficient of variation of Z, and $f_1(b)$ is a function of b [Ref. 5]. Equation (21) indicates that the statistical dispersion of Z diminishes as n increases, and hence the dispersion of R_n, Eq. (6), depends with increasing n mainly on the dispersion of the initial resisting stress R_0. This indicates the importance of taking into account the statistical variation of the material strength.

Thus the Poisson failure rate $h_p(n)$ follows from Eqs. (8), (14), and (16) as

$$h_p(n) = \int_0^\infty (x\sigma_n\sqrt{2\pi})^{-1} \exp\left\{-\left[\frac{x^2}{2\sigma_S^2}\right] - \left[\frac{(\ln x - \mu_n)^2}{2\sigma_n^2}\right]\right\} dx \tag{22}$$

Once $h_p(n)$ is computed, the reliability $L(N)$ can be obtained from either Eq. (12) or (13) by replacing $h(n)$ by $h_p(n)$.

It should be noted that the particular choice of log-normality for R_0 is not essential here. Any other distribution can be used if there is reason to believe that it represents the material better.

From physical reasoning, it is appropriate to assume that the correlation coefficient $\rho(mT_0)$ of the responses $S(t)$ and $S(t+mT_0)$ decreases monotonically to zero with increasing m, i.e.,

$$\rho(m_1 T_0) > \rho(m_2 T_0)$$

for $m_2 > m_1$, and $\rho(mT_0) \to 0$ as $m \to \infty$. This assumption is obviously satisfied, for example, by the response process of a single-degree-of-freedom oscillator excited by white noise. Therefore, the following important properties of the stationary point process $\{S_n^b\}$, can be obtained from Eqs. (10), (18), and (19).

$$\left.\begin{aligned} &\sigma_z^2 \sim n\sigma \quad ; \quad \sigma < \infty \\ &E[|S_j^b|^{2+\delta}] < \infty \quad ; \quad \delta > 0 \\ &E[S_j^b S_{j+m}^b] - E[S_j^b]\,E[S_{j+m}^b] \to 0 \quad \text{as } m \to \infty \\ &E[S_j^b S_{j+m}^b] > E[S_j^b S_{j+\ell}^b] \quad \text{for } \ell > m \end{aligned}\right\} \tag{23}$$

Since Eq. (23) satisfies conditions for a stationary point process $\{S_n^b\}$ to have asymptotic normality (Refs. 14 and 15), i.e., the sum of $S_j^b; j = 1, 2, \cdots, n$, tends to be asymptotically normal for increasing n. Z is therefore asymptotically normal.

b. Clump size approximation. A useful concept was suggested by Lyon (Ref. 16) that the level crossings by $S(t)$ are not independent but tend to occur in clumps of dependent crossings. For the narrow-band random process, since each positive upward level crossing by $S(t)$ results in a peak, the events that the peaks, $S_j; j=1, 2, \cdots$, exceeding a threshold level are not independent but tend to occur in clumps. The Poisson assumption implies that one clump of peaks being above the threshold level constitutes only one peak (Footnote 1). Hence, if clumps are assumed to occur independently, the average failure rate denoted by $\bar{h}(n)$ follows from Eq. (22) as

$$\bar{h}(n) = \int_0^\infty \{x\sigma_n \sqrt{2\pi} E[M|x]\}^{-1} \exp\left\{-\left[\frac{x^2}{2\sigma_S^2}\right] - \left[\frac{(\ln x - \mu_n)^2}{2\sigma_n^2}\right]\right\} dx \tag{24}$$

in which $E[M|x]$ is the average clump size given that the barrier level is equal to x. The structural reliability based on clump size approximation can then be obtained from Eq. (12) by replacing $h(n)$ by $\bar{h}(n)$.

The approximate estimation of $E[M|x]$ has been given in Footnote 1 as follows:

$$E[M|x] \simeq 1 + \sum_{m=1}^{\infty} \frac{m(q_m - q_{m+1})}{q_0} \tag{25}$$

in which

$$q_0 = P[S_j \geqq x] = \exp\left(\frac{-x^2}{2\sigma_S^2}\right) \tag{26}$$

$$q_m = P[S_j \geqq x, S_{j+m} \geqq x] = \int_x^\infty \int_x^\infty f_S(y, z; mT_0)\, dy\, dz \tag{27}$$

with $f_S(y, z; mT_0)$ given by Eq. (10).

5. Effect of Loading History and Other Flaw Propagation Law

It can be observed from Eqs. (6), (7), and (11) that the effect of loading history (or sequence) on the structural reliability is accounted for which, however, cannot be accomplished using the cumulative damage hypothesis and the Palmgren–Miner rule. This is one of the advantages of the flaw propagation approach.

For another flaw propagation law, e.g., $b = 3$ or 4, a similar approach (discussed above) can be applied to find failure rates $h_p(n)$ and $\bar{h}(n)$ and hence the structural reliability $L(N)$.

6. Numerical Example

Making the transformation $\gamma = x/\sigma_S$, the average failure rate $\bar{h}(n)$ given in Eq. (24) can be written as

$$\bar{h}(n) = \frac{1}{\sqrt{2\pi}} \int_0^\infty \frac{1}{\gamma\sigma_n E[M|\gamma\sigma_S]} \times \exp\left\{-\frac{\gamma^2}{2} - \frac{1}{2}\left[\frac{\ln\left(\frac{\gamma\sqrt{V_0^2+1}}{\nu_0}\right) + \mu_z}{\sigma_n}\right]^2\right\} d\gamma \tag{28}$$

in which

$$V_0 = [\exp(\sigma_0^2) - 1]^{1/2}$$

is the coefficient of variation of R_0, and $\nu_0 = \bar{R}_0/\sigma_S$ is the normalized initial barrier level with $\bar{R}_0$ the mean value of

R_0. ν_0 is related to a central safety factor ν_c as, $\nu_c = \bar{R}_0/\mu_S = \nu_0\sqrt{2/\pi}$, where μ_S is the mean value of S_n. Since ν_c is based on the central measures of location of R_0 and S_n, it is called central safety factor, which plays a major role in the reliability-based optimum structural design (Refs. 8–10, Footnote 2). In deriving Eq. (28), the relationship

$$\mu_0 = \ln\left(\frac{\bar{R}_0}{\sqrt{V_0^2+1}}\right)$$

associated with the log-normal distribution of R_0 has been employed.

With the aid of Eqs. (16), (17), and (20), σ_n and μ_z appearing in Eq. (28) can be written as follows:

$$\mu_z = \frac{n}{2} C_p \left(\frac{\sqrt{2}}{\nu_0}\right)^b \Gamma\left(1+\frac{b}{2}\right) \tag{29}$$

$$\sigma_n^2 = \ln(V_0^2+1) + \frac{n}{4\zeta} C_p^2 \left(\frac{\sqrt{2}}{\nu_0}\right)^{2b} \Gamma^2\left(1+\frac{b}{2}\right) f_1(b) \tag{30}$$

where $C_p = K\bar{R}_0^b$ is a flaw propagation factor depending on the particular material and environmental conditions.

It follows from Eqs. (28), (29), and (30) that the average failure rate, and hence the structural reliability, are characterized by C_p, V_0 and ν_0, where C_p and V_0 are material properties associated with flaw propagation and initial strength dispersion (or initial flaw size dispersion), and ν_0 is the normalized initial barrier level (or a measure of the central safety factor) relating the applied load characteristics to the structural design.

Consider a simple structure, that can be idealized as a single-degree-of-freedom system, excited by white noise, $n(t)$, where the displacement $Y(t)$ is related to $n(t)$ as follows:

$$\ddot{Y}(t) + 2\zeta\omega_n \dot{Y}(t) + \omega_n^2 Y(t) = n(t) \tag{31}$$

The stress response process $S(t)$ is related to $Y(t)$ by $S(t) = DY(t)$, with D being a suitable constant.

To show the relationship of ν_0, or of the central safety factor, $\nu_c = \nu_0\sqrt{2/\pi}$, to the structural design and to the applied load characteristics, the simple structure consisting of a mass M supported by a beam with area A_1, length L and Young's modulus of elasticity E is considered. It can easily be shown that ω_n appearing in Eq. (31) is $\omega_n^2 = A_1E/ML$ and

$$\sigma_S^2 = \frac{\phi_0 \pi E^2}{2\zeta\omega_n^3 L^2}$$

where ϕ_0 is the mean square spectral density of white noise $n(t)$. Hence,

$$\nu_0 = \bar{R}_0 \left(\frac{2\zeta}{\pi\phi_0}\right)^{1/2} \left(\frac{A_1}{M}\right)^{3/4} \left(\frac{L}{E}\right)^{1/4} \tag{32}$$

In the present example, it is assumed that failure is due to tension only. The damping coefficient is assumed 0.02.

Failure rates $h_p(n)$ associated with different values of C_p, V_0 and ν_0 are plotted in Fig. 1. In Fig. 1(a), $C_p = 0$, representing the case where the fatigue failure mode is neglected, and hence failure rates are constant. In Figs. 1(b) and 1(c) failure rates are plotted versus the number of stress cycles n. It is clearly shown in Fig. 1 that for this example: (1) because of the interaction of the fatigue failure mode, the failure rate increases monotonically with respect to n and C_p; (2) the failure rate increases as the statistical dispersion, V_0, of the initial material strength, R_0, increases; and (3) the effect of the fatigue failure mode is negligible for small n justifying the assumption of normality for the random variable Z, Eqs. (7) and (16).

In Fig. 2, the structural reliability $L(N)$, based on clump size approximation, is plotted as a function of stress cycles N. It is observed from Fig. 2 that neglecting the effect of the fatigue failure mode, i.e., $C_p = 0$, results in an unconservative reliability prediction. This situation becomes much more critical as the flaw propagation factor C_p increases. It is further observed that the structural reliability decreases as the statistical dispersion V_0 of the material strength R_0 increases. This reflects an important fact that overlooking the statistical variation of material strength results in an unsafe design.

Although a particular flaw propagation law, $b = 2$, and a particular distribution function (log normal) for the initial material strength R_0, are used in the numerical example, above trends of observations are believed to hold for other flaw propagation laws such as $b = 3$ or $b = 4$, as well as other statistical distribution functions for R_0.

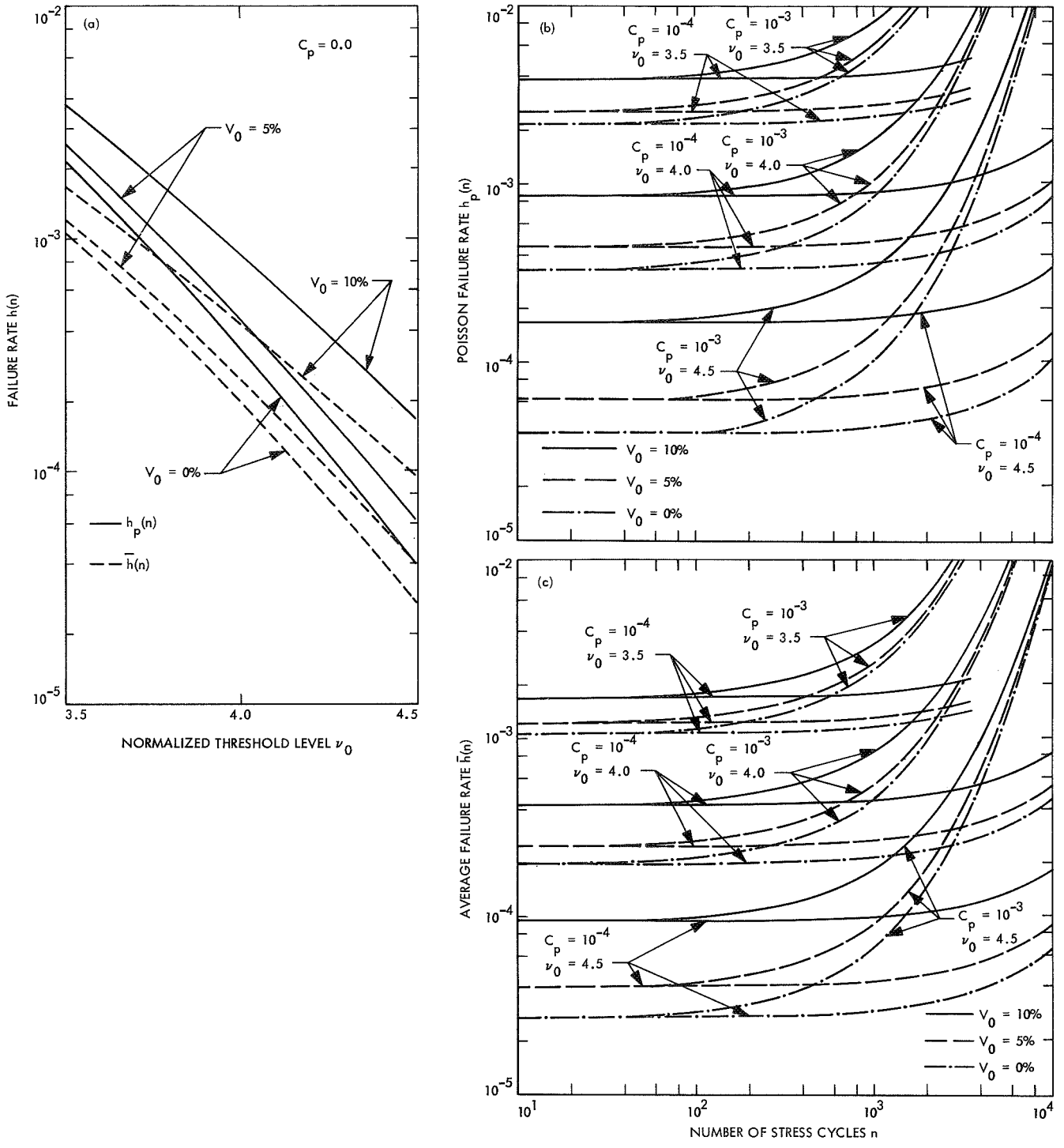
(a)
$C_p = 0.0$
V_0 = 5%
V_0 = 10%
V_0 = 0%
$h_p(n)$
$\bar{h}(n)$
FAILURE RATE h(n)
NORMALIZED THRESHOLD LEVEL ν_0
(b)
POISSON FAILURE RATE $h_p(n)$
$C_p = 10^{-4}$, $\nu_0 = 3.5$
$C_p = 10^{-3}$, $\nu_0 = 3.5$
$C_p = 10^{-4}$, $\nu_0 = 4.0$
$C_p = 10^{-3}$, $\nu_0 = 4.0$
$C_p = 10^{-3}$, $\nu_0 = 4.5$
$C_p = 10^{-4}$, $\nu_0 = 4.5$
V_0 = 10%
V_0 = 5%
V_0 = 0%
(c)
AVERAGE FAILURE RATE $\bar{h}(n)$
$C_p = 10^{-4}$, $\nu_0 = 3.5$
$C_p = 10^{-3}$, $\nu_0 = 3.5$
$C_p = 10^{-4}$, $\nu_0 = 4.0$
$C_p = 10^{-3}$, $\nu_0 = 4.0$
$C_p = 10^{-4}$, $\nu_0 = 4.5$
$C_p = 10^{-3}$, $\nu_0 = 4.5$
V_0 = 10%
V_0 = 5%
V_0 = 0%
NUMBER OF STRESS CYCLES n

Fig. 1. Failure rates $h_p(n)$ and $\bar{h}(n)$: (a) Constant failure rates $h_p(n)$ and $\bar{h}(n)$ for $C_p = 0.0$, (b) Poisson failure rate $h_p(n)$ versus number of stress cycles n, (c) Average failure rate $\bar{h}(n)$ based on the clump size approximation versus number of stress cycles n

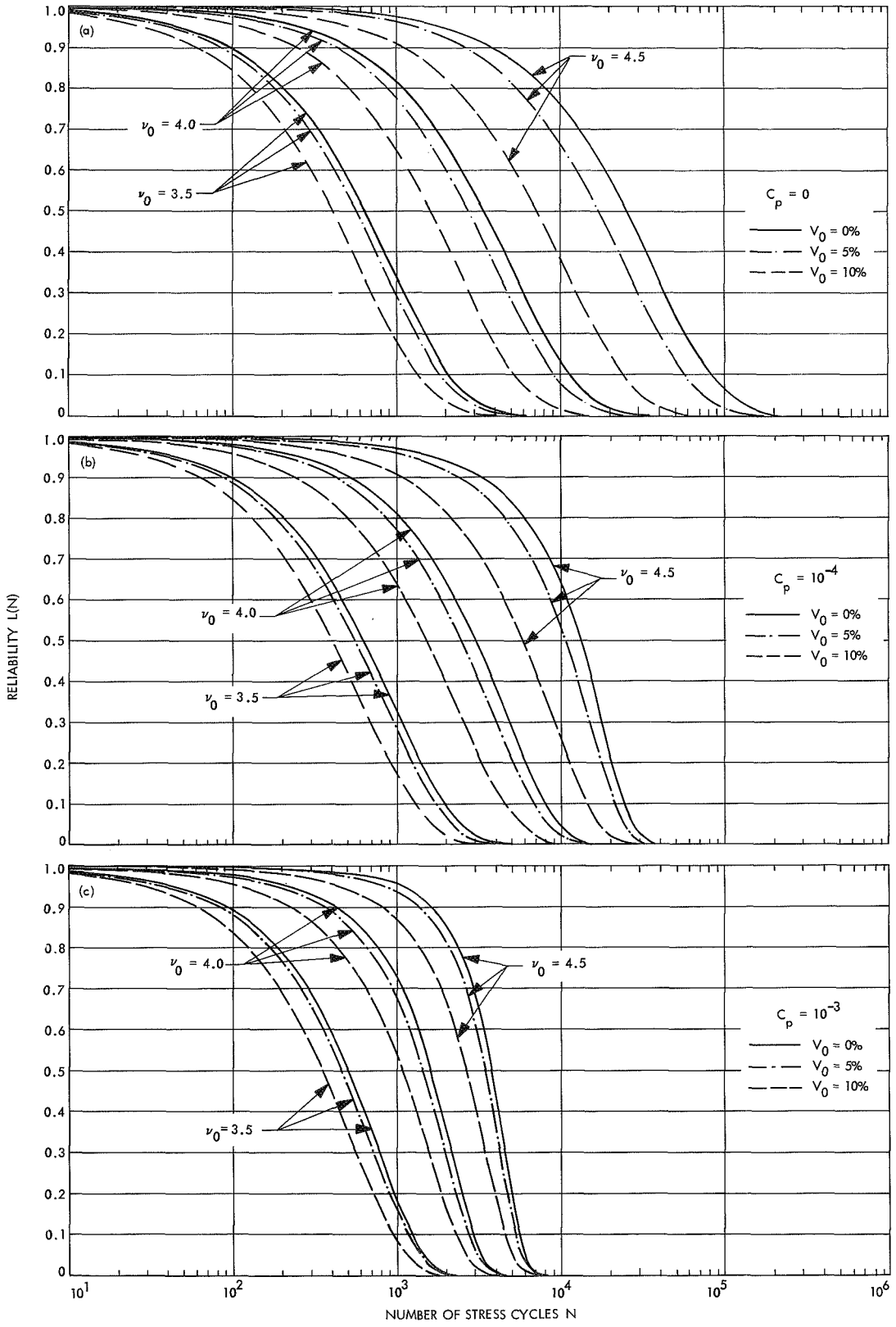

Fig. 2. Structural reliability *L (N)* versus number of stress cycles *N*: (a) $C_p = 0$, (b) $C_p = 10^{-4}$, (c) $C_p = 10^{-3}$

References

1. Heer, E., and Trubert, M., "Analysis of Space Vehicle Structures Using the Transfer-Function Concept," Technical Report 32-1367, Jet Propulsion Laboratory, Pasadena, Calif., April 1, 1969.

2. Yang, J.-N., and Shinozuka, M., "First-Passage Time Problem," *J. Acoust. Soc. Amer.*, Vol. 47, No. 1 (Part II), pp. 393–394, Jan. 1970.

3. Lin, Y. K., "Random Process," *J. Appl. Mech. Rev.*, Sept. 1969.

4. Crandall, S. H., "First Crossing Probabilities of the Linear Oscillator," *J. Sound Vib.*, Vol. 12, No. 3, pp. 285–299, July 1970.

5. Crandall, S. H., Mark, W. D., and Khabbaz, G. R., "The Variance in Palmgren–Miner Damage due to Random Vibration," *Proceedings of the 4th U.S. National Congress of Applied Mechanics*, Vol. I, pp. 119–126, 1962.

6. Shinozuka, M., and Yang, J.-N., "Nonstationary Peak Distribution," *Proceedings of the ASCE-EMD Specialty Conference on Probabilistic Concepts and Methods in Engineering*, pp. 169–173, Purdue University, Nov. 1969.

7. Smith, S. H., "Fatigue Crack Growth Under Axial Narrow and Broad Band Random Loading," in *Acoustical Fatigue in Aerospace Structures*, pp. 331–360. Edited by Trapp, J. W., and Forney, P. M., Syracuse University Press, 1965.

8. Shinozuka, M., and Yang, J.-N., "Optimum Structural Design Based on Reliability and Proof Load Test," *Ann. Assur. Sci.*, Vol. 8, pp. 375–391, 1969.

9. Shinozuka, M., Yang, J.-N., and Heer, E., "Optimum Structural Design Based on Reliability Analysis," *Proceedings of the Eighth International Symposium on Space Technology and Science*, pp. 245–258, Tokyo, Japan, Aug. 1969.

10. Heer, E., and Yang, J.-N., "Optimum Pressure Vessel Design Based on Fracture Mechanics and Reliability Criteria," *Proceedings of the ASCE-EMD Specialty Conference on Probabilistic Concepts and Methods in Engineering*, Purdue University, Nov. 1969, pp. 102–106.

11. Liu, H. W., "Fatigue Crack Propagation and Applied Stress Range–An Energy Approach," *J. Bas. Engin.*, ASME, Vol. 85, pp. 116–122, 1963.

12. Paris, P., and Erdogan, F., "A Critical Analysis of Crack Propagation Laws," *J. Bas. Engin.*, ASME, Vol. 85, No. 4, pp. 528–543, Dec. 1963.

13. Rice, S. O., "Mathematical Analysis of Random Noise," in *Selected Papers on Noise and Stochastic Processes*. Edited by N. Wax, Dover Pub., N.Y., 1955.

14. Sherfling, R. J., "Contribution to Central Limit Theory for Dependent Variables," Institute of Statistics Mimeo No. 514, Department of Statistics, University of North Carolina, Chapel Hill, N.C., March 1967, p. 42.

15. Ibragimov, I. A., "Some Limit Theorems for Stationary Process," *Theor. Prob. Appl.*, Vol. 7, 1962, pp. 349–382.

16. Lyon, R. H., "On the Vibration Statistics of a Randomly Excited Hard-Spring Oscillator II," *J. Acoust. Soc. Amer.*, p. 33, 1961.

C. Boundary Layer Equations of a Heated Constrained Spherical Shell, *H. E. Williams*[1]

1. Introduction

The general equations governing the nonlinear, thermoelastic behavior of thin shells of revolution derived earlier by the author[2] can be vastly simplified when applied to specific cases. It is the purpose of this article to investigate the limiting form of these equations when the shell is thin enough for a boundary layer to develop. The range of the temperature distribution studied here is expressly taken such that the order of magnitude of the resulting transverse deflection is comparable with the thickness of the shell. This range is well above that appropriate for small deflection theory, and should establish a range of temperatures within which these simpler theories are applicable. The boundary layer equations are developed first for a general asymmetric displacement field and then applied to the case of a uniformly heated shallow spherical shell.

[1]Consultant, Harvey Mudd College, Claremont, Calif.

[2]Williams, H. E., "On the Thermoelastic Equations of Thin Shells of Revolution," submitted to *Journal of Solids and Structures*.

2. Analysis of Edge Region

At this stage, it will be assumed that the shell (Fig. 1) is spherical with radii of curvature R and heated uniformly through the thickness to a temperature whose

distribution is $T_0(\phi, \theta)$. The order of magnitude of the temperature is measured by the parameter T^* where

$$T_0 = T^* \cdot \bar{T}_0 \qquad \bar{T}_0, a\frac{\partial \bar{T}_0}{\partial r}, \frac{\partial \bar{T}_0}{\partial \theta} = 0(1)$$

The thermal strain parameter αT^* is measured relative to h/R through the parameter H such that

$$H = \sqrt{3(1-\nu^2)} \cdot \frac{\alpha T^*}{h/R} = 0(1)$$

Further, it will be assumed that

$$h/R << 1$$

$$\frac{a}{R} < 1$$

$$\frac{Rh}{a^2} << 1$$

It should be noted that a uniform temperature corresponding to $H = 0(1)$ in a shell for which $Rh << a^2$ is much larger than that

$$(\alpha T_{crit} \approx h^2/a^2)$$

sufficient to cause buckling of a flat, circular plate of the same thickness h and span a. For this reason, it is expected that a boundary layer will develop with a width comparable to that predicted by linear theory. This suggests using a boundary layer coordinate ξ such that

$$\frac{r}{a} = 1 + \epsilon\xi = x$$

$$\epsilon^2 = \frac{Rh/a^2}{\sqrt{3(1-a^2)}}$$

and

$$\frac{\partial(\ )}{\partial \phi} = \frac{R\cos\phi}{\epsilon a} \cdot \frac{\partial(\ )}{\partial \xi}$$

Thus, in terms of the following dimensionless displacements,

$$(w_1, U_1, U_2) = \alpha RT^* \cdot \left[\bar{w}(\xi, \theta), \frac{\epsilon a}{R} \cdot \bar{U}_1(\xi, \theta), \frac{\epsilon^2 a}{R} \cdot \bar{U}_2(\xi, \theta)\right]$$

$$\epsilon_m = \alpha T^* \cdot \bar{\epsilon}_m(\xi, \theta)$$

rotations,

$$\beta_1 = \frac{\alpha RT^*}{\epsilon a} \cdot \bar{\beta}_1 \qquad \beta_2 = \frac{\alpha RT^*}{a} \cdot \bar{\beta}_2$$

and, stress resultants

$$N_\phi = Eh\alpha T^* \cdot \epsilon \bar{N}_r$$

$$N_\theta = Eh\alpha T^* \cdot \bar{N}_\theta$$

$$N_{\phi\theta} = Eh\alpha T^* \cdot \epsilon \bar{N}_{r\theta}$$

$$M_{\phi\theta} = \frac{Eh^2\alpha T^*}{\sqrt{3(1-\nu^2)}} \cdot \epsilon \bar{M}_{r\theta}$$

$$(M_\phi, M_\theta) = \frac{Eh^2\alpha T^*}{\sqrt{3(1-\nu^2)}} \cdot (\bar{M}_r, \bar{M}_\theta)$$

$$Q_\phi = \frac{Eh^2\alpha T^*}{\epsilon a\sqrt{3(1-\nu^2)}} \cdot \bar{Q}_r$$

$$Q_\theta = \frac{Eh^2\alpha T^*}{a\sqrt{3(1-\nu^2)}} \cdot \bar{Q}_\theta$$

$$S = \frac{Eh^2\alpha T^*}{R} \cdot \bar{S}$$

the equation of Footnote 2 reduce to the following displacement-stress resultant equations

$$\bar{\beta}_1 + \frac{\partial \bar{w}}{\partial \xi} \cdot \cos\phi_0 = 0 \qquad \bar{\beta}_2 + \frac{\partial \bar{w}}{\partial \theta} = 0$$

$$\frac{\partial \bar{U}_1}{\partial \xi} \cdot \cos\phi_0 + \bar{w} + \frac{H}{2} \cdot \cos^2\phi_0 \cdot \left(\frac{\partial \bar{w}}{\partial \xi}\right)^2 + \nu \bar{N}_\theta = \bar{T}_0(a, \theta)$$

$$\bar{w} - \bar{N}_\theta = \bar{T}_0(a, \theta)$$

$$\cos\phi_0 \cdot \frac{\partial \bar{U}_2}{\partial \xi} + \frac{\partial \bar{U}_1}{\partial \theta} + H \cdot \cos\phi_0 \cdot \frac{\partial \bar{w}}{\partial \xi} \cdot \frac{\partial \bar{w}}{\partial \theta} = a \cdot (1+\nu) \cdot \bar{N}_{r\theta}$$

$$\frac{1-\nu^2}{4} \cdot \frac{\partial \bar{\beta}_1}{\partial \xi} \cdot \cos\phi_0 - (\bar{M}_r - \nu \bar{M}_\theta) = 0$$

$$\bar{M}_\theta - \nu \bar{M}_r = 0$$

$$\bar{\epsilon}_m + \frac{H}{2} \cdot \bar{\beta}_1^2 + \nu \bar{N}_\theta = \bar{T}_0(a, \theta)$$

$$\cos\phi_0 \cdot \frac{\partial \bar{\beta}_2}{\partial \xi} + \frac{\partial \bar{\beta}_1}{\partial \theta} = \frac{8}{1-\nu} \cdot \bar{M}_{r\theta}$$

and equations of equilibrium

$$\frac{\partial \bar{N}_r}{\partial \xi} - \bar{N}_\theta = 0$$

$$\cos\phi_0 \cdot \frac{\partial \bar{N}_{r\theta}}{\partial \xi} + \frac{\partial \bar{N}_\theta}{\partial \theta} = 0$$

$$\cos\phi_0 \cdot \frac{\partial \bar{Q}_r}{\partial \xi} - \bar{N}_\theta = 0$$

$$\cos\phi_0 \cdot \frac{\partial \bar{M}_r}{\partial \xi} - \bar{Q}_r = 0$$

$$\cos\phi_0 \cdot \frac{\partial \bar{M}_{r\theta}}{\partial \xi} + \frac{\partial \bar{M}_\theta}{\partial \theta} - \bar{Q}_\theta = 0$$

$$\sqrt{3(1-\nu^2)} \cdot \bar{S} + H \cdot \cos\phi_0 \times \left[\bar{Q}_r \frac{\partial \bar{w}}{\partial \xi} - \cos\phi_0 \cdot \frac{\partial}{\partial \xi}\left(\bar{M}_r \cdot \frac{\partial \bar{w}}{\partial \xi}\right)\right] + \bar{M}_r + \bar{M}_\theta = 0$$

---

it follows that

$$\bar{N}_\theta = \bar{w} - \bar{T}_0(a,\theta)$$

$$\cos\phi_0 \cdot \frac{\partial \bar{N}_{r\theta}}{\partial \xi} = \frac{\partial}{\partial \theta}\left[\bar{T}_0(a,\theta) - \bar{w}\right]$$

$$\frac{\partial \bar{N}_r}{\partial \xi} = \bar{w} - \bar{T}_0(a,\theta)$$

$$\bar{M}_r = -\frac{\cos^2\phi_0}{4} \cdot \frac{\partial^2 \bar{w}}{\partial \xi^2} \qquad \bar{M}_{r\theta} = -\frac{1-\nu}{4} \cdot \frac{\partial^2 \bar{w}}{\partial \xi \partial \theta} \cdot \cos\phi_0$$

$$\bar{Q}_r = -\frac{\cos^3\phi_0}{4} \cdot \frac{\partial^3 \bar{w}}{\partial \xi^3} \qquad \bar{Q}_\theta = -\frac{\cos^2\phi_0}{4} \cdot \frac{\partial^3 \bar{w}}{\partial \theta \partial \xi^2}$$

$$\frac{\partial}{\partial \xi} \cdot \left[\bar{U}_1 \cdot \cos\phi_0 + (1+\nu) \cdot \bar{N}_r\right] = -\frac{H}{2} \cdot \cos^2\phi_0 \cdot \left(\frac{\partial \bar{w}}{\partial \xi}\right)^2$$

$$\cos^2\phi_0 \cdot \frac{\partial^2 \bar{U}_2}{\partial \xi^2} = (1+\nu) \cdot \frac{\partial \bar{T}_0}{\partial \theta} - \frac{\partial \bar{w}}{\partial \theta} \cdot \left(1 + \nu + H \cdot \cos^2\phi_0 \cdot \frac{\partial^2 \bar{w}}{\partial \xi^2}\right)$$

---

where

$$\bar{w} = \bar{T}_0(a,\theta) + e^{\bar{\xi}} \cdot \left[C_1(\theta) \cdot \cos\bar{\xi} + C_2(\theta) \cdot \sin\xi\right]$$

in the limit $\epsilon \to 0$, ξ is fixed. Note that

$$\lim_{\substack{\epsilon \to 0 \\ \xi \text{ fixed}}} T_0(r_1,\theta) = T_0(a,\theta) \qquad \text{as} \lim_{\substack{\epsilon \to 0 \\ \xi \text{ fixed}}} r = a$$

The solution of this set of equations depends on the form of $\bar{T}_0(a,\theta)$ and on the particular boundary conditions at $\xi = 0$. Note that all variables may be expressed in terms of $\bar{w}, \bar{T}_0$ where $\bar{w}(\xi,\theta)$ is governed by

$$\frac{\cos^4\phi_0}{4} \cdot \frac{\partial^4 \bar{w}}{\partial \xi^4} + \bar{w} = \bar{T}_0(a,\theta)$$

Thus, with

$$\bar{\xi} = \frac{\xi}{\cos\phi_0}$$

Note that it is only the in-plane displacements $(\bar{U}_1, \bar{U}_2)$ that are nonlinearly dependent on the temperature distribution. It should be noted further that these equations

are similar to those proposed by Wittrick (Ref. 1) as applicable for small deflections.

3. Uniformly Heated Shell

The solution presented above is valid in the region near the edge. Before it can be completely defined, the behavior of the solution in the interior region must be established. The final form of the solution is determined from the requirement that the solution match in an intermediate region.

As an example of the use of the solution for the edge region—the inner solution—let us consider the particular case of a uniform temperature distribution in a shallow spherical shell, i.e.

$$\bar{T}_0 = 1 \qquad \cos\phi_0 \approx 1$$

As the problem becomes axisymmetric, the functions of integration $[c_1(\theta), c_2(\theta)]$ become constants and we obtain

$$\bar{w} = 1 + e^{\xi} \cdot (c_2 \sin\xi - \cos\xi)$$

for the inner transverse deflection satisfying the condition that $\bar{w}(0) = 0$. The corresponding in-plane deflection becomes

$$\bar{U}_1 = -(1+\nu)\cdot\bar{N}_r - \frac{H}{8}\cdot e^{2\xi}\cdot[2\cdot(c_2^2+1) + (1-2c_2-c_2^2)\cdot\cos 2\xi + (c_2^2-2c_2-1)\cdot\sin 2\xi] + c_3$$

Also

$$\bar{N}_r = -\frac{e^{\xi}}{2}\cdot[(1-c_2)\cdot\sin\xi + (1+c_2)\cdot\cos\xi]$$

A constant of integration is not required for the radial stress resultant $\bar{N}_r$ as it can be shown that

$$\bar{Q}_r \cdot \cos\phi_0 = N_r$$

for a finite segment of the shell to be in vertical equilibrium in the absence of distributed surface pressure, and

$$\bar{Q}_r = -\frac{1}{4}\cdot\frac{\partial^3 w}{\partial\xi^3}$$

The constant c_2 is determined by the choice of edge fixity, i.e., either

$$\frac{\partial\bar{w}}{\partial\xi}(0) = 0 \qquad c_2 = 1 \qquad \text{(clamped)}$$

$$\bar{M}_r(0) = 0 \qquad c_2 = 0 \qquad \text{(simply supported)}$$

With the constant c_2 fixed, c_3 is determined by the requirement $\bar{U}_1(0) = 0$, that is

$$c_3 = -\frac{1+\nu}{2}\cdot(1+c_2) + \frac{H}{8}\cdot(c_2^2 - 2c_2 + 3)$$

In summary, we obtain the following behavior as $\xi \to -\infty$:

$$\bar{w} \to 1 \qquad \bar{N}_r \to 0 \qquad \bar{U}_1 \to c_3 \neq 0$$

Noting that $\bar{U}_1$ does not vanish away from the edge, the solution in the interior of the shell—the outer solution —will be assumed to be that corresponding to a uniform, stress-free dilation plus a vertical rigid body translation of magnitude δ, i.e.,

$$U_1 = -\delta\cdot\sin\phi \qquad U_2 = 0 \qquad \epsilon_m = \alpha T_0$$

$$= -\delta\alpha x/R$$

$$N_\phi, N_\theta; M_\phi, M_\theta, Q_r = 0$$

$$w = \alpha R T_0 + \delta\cdot\cos\phi \approx \alpha R T_0 + \delta$$

Note that $\delta = \delta(\epsilon)$ at this stage.
Matching of the two solutions is accomplished by requiring

$$\lim_{\substack{\epsilon\to 0 \\ \xi \text{ fixed}}}\left[c_3 + \frac{\delta(\epsilon)\cdot x}{\epsilon\alpha T^* R}\right] = 0$$

that is

$$\delta = -\epsilon\cdot c_3\cdot\alpha R T^*$$

Thus, the first order composite solution for the displacements can be written

$$\bar{w} = 1 + e^{\xi} \cdot (c_2 \cdot \sin \xi - \cos \xi)$$

$$\bar{U}_1 = -(1 + \nu) \cdot \bar{N}_r - \frac{H}{8} \cdot e^{2\xi} \cdot [2 \cdot (c_2^2 + 1) + (1 - 2c_2 - c_2^2) \cdot \cos 2\xi + (c_2^2 - 2c_2 - 1) \sin 2\xi] + x\left[-\frac{1 + \nu}{2} \cdot (1 + c_2) + \frac{H}{8} \cdot (c_2^2 - 2c_2 + 3)\right]$$

where

$$c_2 = 1 \qquad \text{(clamped)}$$

or

$$c_2 = 0 \qquad \text{(simply supported)}$$

4. Discussion

It should be noted that the equations derived above are essentially linear. The in-plane deflections ($\bar{U}_1, \bar{U}_2$) are exceptions, but have no effect on the stress distribution. Thus, the behavior of the stresses and transverse deflection is similar to that predicted by linear theory, even when the transverse deflection is much greater than that considered appropriate for linear theory.

That the transverse deflection is linear in the temperature should not be surprising as it has been predicted by Reissner (Ref. 2) that one should not expect nonlinearity to be important until the transverse deflection is of the order of the boundary layer thickness ($\sqrt{Rh}$). The magnitude studied here was of the order of the shell thickness as $\alpha RT^* = h \cdot 0\,(1)$. Note that Reissner's analysis assumed a set of equations shown earlier to be generally applicable, whereas the principal object of this note was to simplify equations considered unnecessarily general for the type of problem studied above.

The boundary layer equations presented above have been derived for spherical shells. In the general form, no restriction was made on the range of the opening angle (ϕ_0), i.e., the shell was not required to be shallow. Obviously, these results are not applicable for deep shells for which $\cos \phi_0$ is small. [This range of shells has been studied by Wittrick (Ref. 3) for a non-shallow shell of arbitrary shape.]

For shallow spherical shells ($\cos \phi_0 \approx 1$), the results presented above may be considered to apply to more general shells of revolution, as ellipsoidal shells of revolution are spherical within an error comparable to that incurred in writing $\cos \phi \approx 1$. Thus, the boundary layer equations presented above apply equally well to a wider class of shells of revolution provided the shell is shallow, or to arbitrarily deep spherical shells provided that $\cos \phi_0$ is not small.

References

1. Wittrick, W. H., "Edge Stresses in Thin Shells of Revolution," *Aust. J. Appl. Sci.*, Vol. 8, p. 235, 1957.

2. Reissner, E., "On Influence Coefficients and Non-linearity for Thin Shells of Revolution," *J. App. Mech.*, pp. 69–72, March, 1959.

3. Wiztrick, W. H., "A Non-linear Theory for the Edge Stresses in Thin Shells," *Int. J. Eng. Sci.*, Vol. 2, pp. 155–177.

D. Derivation of the Equations Governing Heated Shallow Shells of Revolution, *H. E. Williams*[1]

1. Introduction

The general equations governing the nonlinear, thermoelastic behavior of thin shells of revolution have been derived by the author[2] using Reissner's Variational Theorem. When applied to specific cases, such as middle surface heating (no temperature gradient through the thickness of the shell) of shallow shells, it is possible to vastly simplify the general equations and obtain the equation generally regarded as Marguerre's equations. It is the purpose of this note to present an order of magnitude analysis of the equations derived in Footnote 2 in order to establish the range of validity of the simpler equations.

2. Analysis

At this stage, it will be assumed that the shell (*Section C*, Fig. 1) is spherical with radii of curvature R and heated uniformly through the thickness to a temperature whose distribution is given by $T_0(\phi, \theta)$. The order of magnitude of the temperature is measured by the parameter T^* such that

$$T_0 = T^* \cdot \bar{T}_0 \qquad \bar{T}_0, a\frac{\partial \bar{T}_0}{\partial r}, \frac{\partial \bar{T}_0}{\partial \theta} = 0(1)$$

The thermal strain parameter (αT^*) is measured relative to (h/a) through the parameter κ such that

$$\kappa = \frac{h^2/a^2}{\alpha T^*} = 0(1)$$

[1]Consultant, Harvey Mudd College, Claremont, Calif.

[2]Williams, H. E., "On the Thermoelastic Equations of Thin Shells of Revolution," submitted to the *Journal of Solids and Structures*.

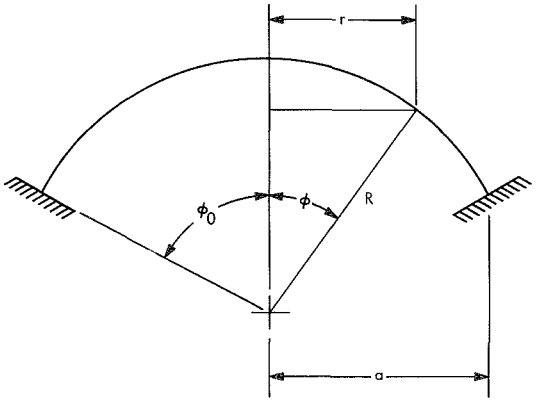

Fig. 1. Coordinate system for a spherical shell

It should be noted that a uniform temperature corresponding to $\kappa = 0(1)$ is sufficient to cause buckling of a flat, circular plate of the same thickness (h) and span (α).

In terms of the variables x, θ where $x = r/a$,

$$\frac{\partial}{\partial \phi}(\ ) = \frac{R\cos\phi}{a} \cdot \frac{\partial(\ )}{\partial x}$$

and the following dimensionless displacements

$$w = h\bar{w}(x, \theta) \qquad (U_1, U_2) = \alpha a T^* \cdot (\bar{U}_1, \bar{U}_2)$$

strain

$$(\epsilon_\phi^{(0)}, \epsilon_\theta^{(0)}, \epsilon_m) = \alpha T^* \cdot (\bar{\epsilon}_\phi, \bar{\epsilon}_\theta, \bar{\epsilon}_m)$$

rotations

$$(\beta_1, \beta_2) = \frac{h}{a} \cdot (\bar{\beta}_1, \bar{\beta}_2)$$

curvatures

$$(\kappa_\phi, \kappa_\theta) = \frac{h}{a^2}(\bar{\kappa}_\phi, \bar{\kappa}_\theta)$$

and stress resultants

$$(N_\phi, N_\theta, N_{\phi\theta}) = Eh\alpha T^* \cdot (\bar{N}_r, \bar{N}_\theta, \bar{N}_{r\theta})$$
$$(M_\phi, M_\theta, M_{\phi\theta}) = Eh^4 \cdot (\bar{M}_r, \bar{M}_\theta, \bar{M}_{r\theta})/(12a^2)$$
$$(Q_1, Q_2) = Eh^4 \cdot (\bar{Q}_r, \bar{Q}_\theta)/(12a^3)$$

the equations presented in Footnote 2 can be vastly simplified. It will be assumed further that

$$\frac{h}{a} << 1 \qquad \frac{a}{R} < 1 \qquad \frac{a^2}{Rh} = 0(1)$$

Within these limitations, the equations of (1) reduce to the following strain-displacement equations

$$\bar{\epsilon}_\phi = \frac{\partial \bar{U}_1}{\partial x} \cdot \cos\phi + \frac{\bar{w}h}{\alpha R T^*}$$

$$\bar{\epsilon}_\theta = \frac{\partial \bar{U}_2}{x\partial\theta} + U_1 \cdot \frac{\cos\phi}{x} + \frac{\bar{w}h}{\alpha R T^*}$$

curvature-displacement equations

$$\bar{\kappa}_\phi = \frac{\partial \bar{\beta}_1}{\partial x} \cdot \cos\phi \qquad \kappa_\theta = \frac{\partial \bar{\beta}_2}{x\partial\theta} + \bar{\beta}_1 \cdot \frac{\cos\phi}{x}$$

displacement-stress resultant equations

$$\bar{\epsilon}_\phi + \frac{\kappa}{2} \cdot \left[\left(\frac{\partial \bar{w}}{\partial x} \cdot \cos\phi \right)^2 + \left(\frac{\bar{w}a}{R} \right)^2 \right] - (\bar{N}_r - \nu \bar{N}_\theta) = \bar{T}_0$$

$$\bar{\epsilon}_\theta + \frac{\kappa}{2} \cdot \left[\left(\frac{\partial \bar{w}}{x \partial \theta} \right)^2 + \left(\frac{\bar{w}a}{R} \right)^2 \right] - (\bar{N}_\theta - \nu \bar{N}_r) = \bar{T}_0$$

$$\bar{\kappa}_\phi - (\bar{M}_r - \nu \bar{M}_\theta) = 0$$

$$\bar{\kappa}_\theta - (\bar{M}_\theta - \nu \bar{M}_r) = 0$$

$$\frac{\partial \bar{U}_1}{x \partial \theta} + \left(\frac{\partial \bar{U}_2}{\partial x} - \frac{\bar{U}_2}{x} \right) \cdot \cos\phi + \frac{\kappa}{x} \cdot \left(\frac{\partial \bar{w}}{\partial x} \cdot \frac{\partial \bar{w}}{\partial \theta} \cdot \cos\phi \right) = 2(1+\nu) \cdot \bar{N}_{r\theta}$$

$$\frac{\partial \bar{\beta}_1}{x \partial \theta} + \left(\frac{\partial \bar{\beta}_2}{\partial x} - \frac{\bar{\beta}_2}{x} \right) \cdot \cos\phi = 2(1+\nu) \cdot \bar{M}_{r\theta}$$

$$\bar{\epsilon}_m + \frac{\kappa}{2} \cdot (\bar{\beta}_1^2 + \bar{\beta}_2^2) + \nu \cdot (\bar{N}_r + \bar{N}_\theta) = \bar{T}$$

$$\bar{\beta}_1 + \frac{\partial \bar{w}}{\partial x} \cdot \cos\phi = 0$$

$$\bar{\beta}_2 + \frac{\partial \bar{w}}{x \partial \theta} = 0$$

and equations of equilibrium

$$-\frac{\cos\phi}{x} \cdot \frac{\partial}{\partial x}(x \bar{M}_r) - \frac{\partial \bar{M}_{r\theta}}{x \partial \theta} + \frac{\bar{M}_\theta}{x} \cdot \cos\phi + Q_r = 0$$

$$-\frac{\cos\phi}{x} \cdot \frac{\partial}{\partial x}(x \bar{M}_{r\theta}) - \frac{\partial \bar{M}_\theta}{x \partial \theta} - \frac{\bar{M}_{r\theta}}{x} \cdot \cos\phi + Q_\theta = 0$$

$$-\frac{\cos\phi}{x} \cdot \frac{\partial}{\partial x}(x \bar{N}_r) - \frac{\partial \bar{N}_{r\theta}}{x \partial \theta} + \bar{N}_\theta \cdot \frac{\cos\phi}{x} = 0$$

$$\cos\phi \cdot \frac{\partial \bar{N}_{r\theta}}{\partial x} + \frac{\partial \bar{N}_\theta}{x \partial \theta} + 2 \cdot \frac{\bar{N}_{r\theta}}{x} \cdot \cos\phi = 0$$

$$\frac{\cos\phi}{x} \cdot \frac{\partial}{\partial x} \left[x \cdot \left(\frac{\kappa \bar{Q}_r}{12} + \bar{N}_r \cos\phi \cdot \frac{\partial \bar{w}}{\partial x} + \bar{N}_{r\theta} \cdot \frac{\partial \bar{w}}{x \partial \theta} \right) \right] + \frac{\partial}{x \partial \theta} \left(\frac{\kappa \bar{Q}_\theta}{12} + \bar{N}_{r\theta} \cdot \frac{\partial \bar{w}}{\partial x} \cdot \cos\phi + \bar{N}_\theta \frac{\partial \bar{w}}{x \partial \theta} \right)$$
$$- \frac{a^2}{Rh} \cdot (\bar{N}_r + \bar{N}_\theta) = 0$$

The transverse normal stress resultant S becomes

$$-\frac{12a^3}{Eh^4} \cdot S = \frac{a}{R} \cdot (\bar{M}_r + \bar{M}_\theta) + \frac{h}{a} \cdot \left\{ \bar{Q}_r \cdot \frac{\partial \bar{w}}{\partial x} \cdot \cos\phi + Q_\theta \cdot \frac{\partial \bar{w}}{x \partial \theta} \right.$$
$$- \frac{\cos\phi}{x} \cdot \frac{\partial}{\partial x} \left[x \cdot \left(\bar{M}_r \cdot \frac{\partial \bar{w}}{\partial x} \cdot \cos\phi + \bar{M}_{r\theta} \cdot \frac{\partial \bar{w}}{x \partial \theta} \right) \right]$$
$$\left. - \frac{\partial}{x \partial \theta} \left(\bar{M}_{r\theta} \cdot \cos\phi \cdot \frac{\partial \bar{w}}{\partial x} + \bar{M}_\theta \cdot \frac{\partial \bar{w}}{x \partial \theta} \right) \right\}$$

The shallow shell equations may be obtained from those given above by writing $\cos\phi \approx 1$ and neglecting $(a/R)^2$ in comparison with unity. If we define

$$\Delta = \frac{\partial^2}{\partial x^2} + \frac{\partial}{x\partial x} + \frac{\partial^2}{x^2\partial\theta^2}$$

the governing equations for a heated, shallow shell become

$$\bar{\beta}_1 = -\frac{\partial \bar{w}}{\partial x} \qquad \bar{\beta}_2 = -\frac{\partial \bar{w}}{x\partial\theta}$$

$$\frac{\partial \bar{U}_1}{\partial x} + \frac{\kappa a^2}{Rh}\cdot\bar{w} + \frac{\kappa}{2}\left(\frac{\partial \bar{w}}{\partial x}\right)^2 - (\bar{N}_r - \nu\bar{N}_\theta) = \bar{T}_0$$

$$\frac{\partial \bar{U}_2}{x\partial\theta} + \frac{\bar{U}_1}{x} + \frac{\kappa a^2}{Rh}\cdot\bar{w} + \frac{\kappa}{2}\left(\frac{\partial \bar{w}}{x\partial\theta}\right)^2 - (\bar{N}_\theta - \nu\bar{N}_r) = \bar{T}_0$$

$$2\cdot(1+\nu)\cdot\bar{N}_{r\theta} = \frac{\partial \bar{U}_1}{x\partial\theta} + \frac{\partial \bar{U}_2}{\partial x} - \frac{\bar{U}_2}{x} + \frac{\kappa}{x}\cdot\frac{\partial \bar{w}}{\partial x}\cdot\frac{\partial \bar{w}}{\partial\theta}$$

$$-(1-\nu^2)\cdot\bar{M}_r = \frac{\partial^2 \bar{w}}{\partial x^2} + \nu\cdot\left(\frac{\partial^2 \bar{w}}{x^2\partial\theta^2} + \frac{\partial \bar{w}}{x\partial x}\right)$$

$$-(1-\nu^2)\cdot\bar{M}_\theta = \frac{\partial^2 \bar{w}}{x^2\partial\theta^2} + \frac{\partial \bar{w}}{x\partial x} + \nu\cdot\frac{\partial^2 \bar{w}}{\partial x^2}$$

$$(1+\nu)\cdot\bar{M}_{r\theta} = -\frac{1}{x}\cdot\frac{\partial^2 \bar{w}}{\partial x\partial\theta} + \frac{1}{x^2}\cdot\frac{\partial \bar{w}}{\partial\theta}$$

$$-(1-\nu^2)\cdot\bar{Q}_r = \frac{\partial(\Delta\bar{w})}{\partial x} \qquad -(1-\nu^2)\cdot\bar{Q}_\theta = \frac{\partial(\Delta\bar{w})}{x\partial\theta}$$

$$\frac{\partial \bar{N}_r}{\partial x} + \frac{\partial \bar{N}_{r\theta}}{x\partial\theta} + \frac{1}{x}(\bar{N}_r - \bar{N}_\theta) = 0$$

$$\frac{\partial \bar{N}_{r\theta}}{\partial x} + \frac{\partial \bar{N}_\theta}{x\partial\theta} + \frac{2}{x}\cdot\bar{N}_{r\theta} = 0$$

$$-\frac{\kappa/12}{1-\nu^2}\cdot\Delta\Delta\bar{w} - \frac{a^2}{Rh}\cdot(\bar{N}_r + \bar{N}_\theta) + \bar{N}_r\cdot\frac{\partial^2 \bar{w}}{\partial x^2}$$

$$+\bar{N}_\theta\cdot\left(\frac{\partial^2 \bar{w}}{x^2\partial\theta^2} + \frac{\partial \bar{w}}{x\partial x}\right) + 2\bar{N}_{r\theta}\cdot\left(\frac{\partial^2 \bar{w}}{x\partial x\partial\theta} - \frac{\partial \bar{w}}{x^2\partial\theta}\right) = 0$$

Often it is convenient to express this system of equations in displacement variables only. Thus, with

---

$$(1-\nu^2)\cdot\bar{N}_r = -(1+\nu)\cdot\bar{T}_0 + \frac{\partial \bar{U}_1}{\partial x} + \nu\cdot\left(\frac{\partial \bar{U}_2}{x\partial\theta} + \frac{\bar{U}_1}{x}\right) + (1+\nu)\cdot\frac{\kappa a^2}{Rh}\cdot\bar{w} + \frac{\kappa}{2}\cdot\left[\left(\frac{\partial \bar{w}}{\partial x}\right)^2 + \nu\cdot\left(\frac{\partial \bar{w}}{x\partial\theta}\right)^2\right]$$

$$(1-\nu^2)\cdot\bar{N}_\theta = -(1+\nu)\cdot\bar{T}_0 + \frac{\partial \bar{U}_2}{x\partial\theta} + \frac{\bar{U}_1}{x} + \nu\cdot\frac{\partial \bar{U}_1}{\partial x} + (1+\nu)\cdot\frac{\kappa a^2}{Rh}\cdot\bar{w} + \frac{\kappa}{2}\cdot\left[\left(\frac{\partial \bar{w}}{x\partial\theta}\right)^2 + \nu\cdot\left(\frac{\partial \bar{w}}{\partial x}\right)^2\right]$$

the in-plane equations of equilibrium become

$$\frac{1-\nu}{2}\cdot\left(\frac{\partial^2 U_2}{\partial r^2} + \frac{\partial U_2}{r\partial r} - \frac{U_2}{r^2}\right) + \frac{\partial^2 U_2}{r^2\partial\theta^2} + \frac{1+\nu}{2r}\cdot\frac{\partial^2 U_1}{\partial r\partial\theta} + \frac{3-\nu}{2r^2}\cdot\frac{\partial U_1}{\partial\theta}$$
$$+\frac{\partial w}{\partial r}\cdot\left(\frac{1+\nu}{2r}\cdot\frac{\partial^2 w}{\partial r\partial\theta} + \frac{1-\nu}{2r^2}\cdot\frac{\partial w}{\partial\theta}\right)$$
$$+\frac{\partial w}{r\partial\theta}\left(\frac{1-\nu}{2}\cdot\frac{\partial^2 w}{\partial r^2} + \frac{1+\nu}{R} + \frac{\partial^2 w}{r^2\partial\theta^2}\right) - \frac{1+\nu}{r}\cdot\frac{\alpha\partial T_0}{\partial\theta} = 0 \qquad (1)$$

$$\frac{\partial^2 U_1}{\partial r^2} + \frac{\partial U_1}{r\partial r} - \frac{U_1}{r^2} + \frac{1-\nu}{2r^2}\cdot\frac{\partial^2 U_1}{\partial\theta^2} + \frac{1+\nu}{2r}\cdot\frac{\partial^2 U_2}{\partial r\partial\theta} - \frac{3-\nu}{2r^2}\cdot\frac{\partial U_2}{\partial\theta}$$
$$+\frac{\partial w}{\partial r}\cdot\left[\frac{1+\nu}{R} + \frac{\partial^2 w}{\partial r^2} + \frac{1-\nu}{2r}\cdot\left(\frac{\partial w}{\partial r} + \frac{\partial^2 w}{r\partial\theta^2}\right)\right]$$
$$+\frac{1+\nu}{2r}\cdot\frac{\partial w}{\partial\theta}\cdot\frac{\partial}{\partial r}\left(\frac{\partial w}{r\partial\theta}\right) - (1+\nu)\cdot\alpha\cdot\frac{\partial T_0}{\partial r} = 0 \qquad (2)$$

The out-of-plane equation may also be written

$$-D\nabla^4 w + N_r \cdot \left(\frac{\partial^2 w}{\partial r^2} - \frac{1}{R}\right) + N_\theta \cdot \left(\frac{\partial^2 w}{r^2 \partial \theta^2} + \frac{\partial w}{r \partial r} - \frac{1}{R}\right) + 2N_{r\theta} \cdot \frac{\partial}{\partial r}\left(\frac{\partial w}{r \partial \theta}\right) = 0 \qquad (3)$$

Equations (1), (2), and (3) have been written in dimensional form for purposes of comparison. In particular, they are identical to those given by Famili and Archer (Ref. 1) as the circular polar form of the equations derived from Marguerre (Ref. 2).

3. Discussion

Although the above equations were expressly derived for a spherical shell, it should be pointed out that they are more generally applicable, as an ellipsoidal shell of revolution is spherical within an error comparable to that involved in writing $\cos\phi \approx 1$. Thus, if (R_1, R_2) are the principal radii of curvature of an ellipsoid with semi-axes (a, b), it may be shown that

$$\frac{R_2}{R_1} = 1 + \frac{a^2 - b^2}{b^2} \cdot \sin^2\phi \approx 1$$

for a shallow shell for which

$$\frac{a^2 - b^2}{b^2} = 0\,(1)$$

As a final remark, it should be noted that the assumption $a^2/Rh = 0\,(1)$ effectively precludes the formation of a boundary layer near the edge $r = a$. This follows from the observation that the thickness of the boundary layer is of order $\sqrt{Rh}$. The assumption is also consistent with the use of (x) as a variable.

References

1. Famili, J., and Archer, R. R., "Finite Asymmetric Deformation of Shallow Spherical Shells," *AIAA Journal*, Vol. 3, No. 3, pp. 506–510.

2. Marguerre, K., "Zur Theorie der Gekrummten Platte Grosser Formanderung," *Proceedings of the Fifth International Congress of Applied Mechanics*, pp. 93–101, 1938.